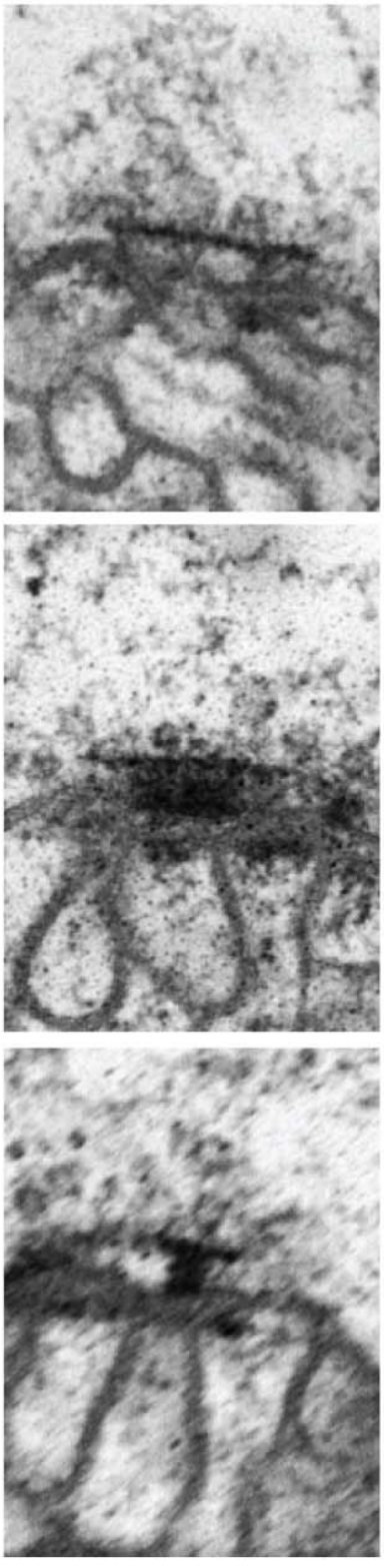

ULTRASTRUCTURE OF SYNAPSES IN DROSOPHILA MELANOGASTER LOBULA PLATE TANGENTIAL CELLS

KRISTINA ENDERS

MÜNCHEN 2011

ULTRASTRUCTURELLE UNTERSUCHUNGEN VON SYNAPSEN AN LOBULAPLATTENTANGENTIALZELLEN VON DROSOPHILA MELANOGASTER

Wissenschaftliche Arbeit zur Erlangung des Grades `Bachelor of Science`

an der Fakultät Biologie der Ludwig-Maximilian-Universität München

Angefertigt am Max-Planck-Institut für Neurobiologie

Abteilung `Neuronale Informationsverarbeitung`

Hiermit versichere ich, dass ich die vorliegende Arbeit selbständig und ohne Benutzung anderer als der angegebenen Hilfsmittel angefertigt, noch nicht einer anderen Prüfungsbehörde vorgelegt und noch nicht veröffentlicht habe.

München, den 30.08.2011

1. Gutachter: Prof. Dr. Alexander Borst

Tag der Präsentation: 8. September 2011

TABLE OF CONTENTS

TABLE OF CONTENT ……..5

1 ABSTRACT……7
2 INTRODUCTION……9

2.1 Motion Vision and Optomotor Response
2.2 Architecture of the Optic Lobes
2.3 Visual System of the Fly
2.4 Reichard type model
2.5 Meeting Point between Neurons - Synaptic Organization in the Fly
2.6 Neuroanatomical Studies and Application of TEM
2.7.1 Goal and Achievements

3 MATERIALS AND METHODS……21

3.1 Specimen Preparation
3.2 Semi Thin Sectioning – The "Atlas of the Optic Lobes"
3.3 Ultra Thin Sectioning
3.4 Transmission Electron Microscopy (TEM)
3.5 Editing Images
3.6 Analyses of the Ultrastructure

4 RESULTS……30

4.1 Semi Thin Sections – – The "Atlas of the Optic Lobes"
4.2 Ultra Thin Sections –Ultrastructure within the Lobula Plate
4.2.1 Overview: STACK 1 and STACK 2
4.2.2 Synapses
4.2.2.1 Typical Synaptic Architecture within Drosophila – Neurites in *Drosophilas* brain
4.2.2.2 High Density of Synapses
4.2.2.3 Connective Terminals,
4.2.2.4 Input and Output
4.2.2.5 Synaptic Vesicles
4.2.2.6 Membran
4.2.2.7 Postsynaptic Density (PSD) and Specializations
4.3 Tables
TABLE 1 STACK 1
TABLE 2 STACK 2
TABLE 3 Postsynaptic Density and Specializations

5 DISCUSSION……54

5.1 Experimental Review
5.2 Analysis Review
5.3 Relative Amount of Synaptic Sites
5.4 Detection of Stereotypy
5.5 Multiple Connections
5.6 PSD
5.7 Relevance for Motion Vision Processing
5.8 Future Prospect

REFERENCES……..62

1 ABSTRACT

Lobula plate tangential cells (LPTCs) play a major role in visual motion processing, based on the optic flow. Information about the synaptic organization within the lobula plate in *Drosophila melanogaster,* is rare.

By using established preparation techniques, sectioning the brain into ultra thin sections and the subsequent visualization by transmission electron microscopy (TEM) revealed the complexity of various synaptic junctions within the lobula plate, where LPTCs are situated. The morphological stereotype synapse, called T bar, was analyzed among two stacks of 3 - 5 successive images of LPTCs. We identified various synaptic sites, which were classified according to the appearance of a dense body, presence of vesicles associated with the presynaptic membrane, a widened synaptic cleft and postsynaptic structures.

We focused at possible structural difference among 17 chemical synaptic connections within the LPTCs to clarify if ultrastructure and synaptic organization can indicate what type of neurotransmitter exchange is present onto LTCPs. According to the traced cells a statistical analysis of the mentioned elements, which indicate synaptic transmission is attached to this study and can subserve for further classification of synaptic sites.

ABSTRAKT

Lobulaplatten- Tangentialzellen (LPTZ) spielen eine wichtige Rolle in der Verarbeitung visueller Bewegungsinformation, basierend auf dem optischen Fluss. Informationen über die synaptische Organisation in der Lobula- Platte von *Drosophila melanogaster*, sind rar.

Unter Verwendung bewährter Präparationstechniken, dem Anfertigten von Ultradünnschnitten des Gehirns und der anschließenden Visualisierung mittels Transmission-Elektronenmikroskopie (TEM) wurde die Komplexität verschiedener synaptischen Verbindungen aus der Lobulaplatte, wo sich diese LPTZ befinden, enthüllt. Die morphologische Stereotyp - Synapse, genannt T-bar, wurde anhand von zwei verschieden Stacks von 3 bis 5 aufeinander folgenden Bildern der LPTZ analysiert. Wir identifizierten verschiedene Synapsen und klassifizierten diese nach folgenden Kriterien: Erscheinung einer prasynaptischen electronendichten Struktur, die Anwesenheit von Vesikel an der präsynaptischen Membran, ein geweiteter synaptischer Spalt und postsynaptische Strukturen.

Unser Hauptaugenmerk lag auf möglichen ultrastrukturellen Unterschieden zwischen 17 chemischen synaptischen Verbindungen an LPTZ, um herauszufinden ob Ultrastruktur und synaptische Organisation den Typ von Neurotransmitter- Austausch an LPTZ anzeigen können. Anhand von den untersuchten LPTZ wurde eine statistische Analyse der genannten Kriterien, welche synaptische Transmission anzeigen, angefertigt, ist der wissenschaftlichen Arbeit angefügt und kann für weitere Klassifikationsstudien von Synapsen dienen.

2 INTRODUCTION

For millions of years, much longer than humans have been living on earth, flies have been searching for mates and food. They developed and optimized a high precision visual control system, which enables them to react to motion physiologically with a time lag of less than 30 ms (Land and Collett, 1974; Wagner 1986). To survive in a world with many obstacles, be it a predator or simply a tree in their way, this system has to function properly.

Flies primarily rely on stimuli of visual nature. However these tiny animals have much better visual course control then humans. Some flies manage acrobatic flight maneuvers with high at speeds up to 3000m/s under high precision. Their spatial resolution is relatively low, because of their size and their direct action. The fly`s eye, which is its most important sensory input organ, is evidence of the success of nature, because they are still buzzing around and hurdling all evolution caused changes of the environment. Their highly adapted concept of visual motion processing is an outstanding optimized system and contributes to why flies are one of the most studied species according to motion vision.

In the fly brain the amount of neuronal hardware dedicated to vision, totals more than half of its entire volume (Strausfeld, 1976). Compared to the vertebrate`s nervous system which contains billions of nerve cells, the fly brain has only a total amount of 100.000 (*Drosophila*) neurons. It is of great interest to understand the whole underlying circuit within the fly`s brain, motion vision is one task the visual system has to perform.

This performance is realized within the complexity of a neuronal network located in the optic lobes of the fly.

2.1 Motion Vision and Optomotor Response

Navigation through the world from the flies' point of view means the permanent avoidance of obstacles, even at exceptionally high speeds. Once airborne, this behavioral reaction is needed to navigate through its world – called visual course control.

If the fly is moving itself, images of the environment are shifted on the retina. The concomitant distribution of motion vectors is called optic flow (Gibson, 1950) and result as a compensatory optomotor response. In particular, optic flow depends on the type of ego-motion as well as on the three- dimensional structure of the surroundings, enabling to differ between nearby and more distant objects. The so called optomotor behavior is thought to be controlled by the large field motion sensitive cells- lobula plate tangential cells (LPTCs), (Borst et al., 2009).

Despite precise specifications of the computational steps of motion vision, the presynaptic input mechanism to the LPTCs still needs to be studied. Motion sensitive tangential cells have often been described with respect to their visual response properties and the connectivity amongst them. The precise function of cells in the lobula plate and descending neurons for visual course control has still to be studied.

2.2 Architecture of the Optic Lobes

The most prominent sensory organs, the eyes, are on both sides of the head. Each visual ganglia behind the retina connects to the central brain and further to the thoracic ganglion. The insect nervous system is composed of a head ganglion, three thoracic ganglia and several abdominal ganglia. In *Drosophila*, the three thoracic and abdominal ganglia are fused into one thoracic ganglion, which is connected to the head ganglia. The connective between these ganglia houses roughly 3600 descending and ascending neurons, the junctions for visual inducted motion (A. Borst, 2009). Anatomical studies revealed the layout of the optical lobes of the fly (Cajal, S. R., 1905; Fischbach and Dittrich,1989;Strausfeld, 1976).

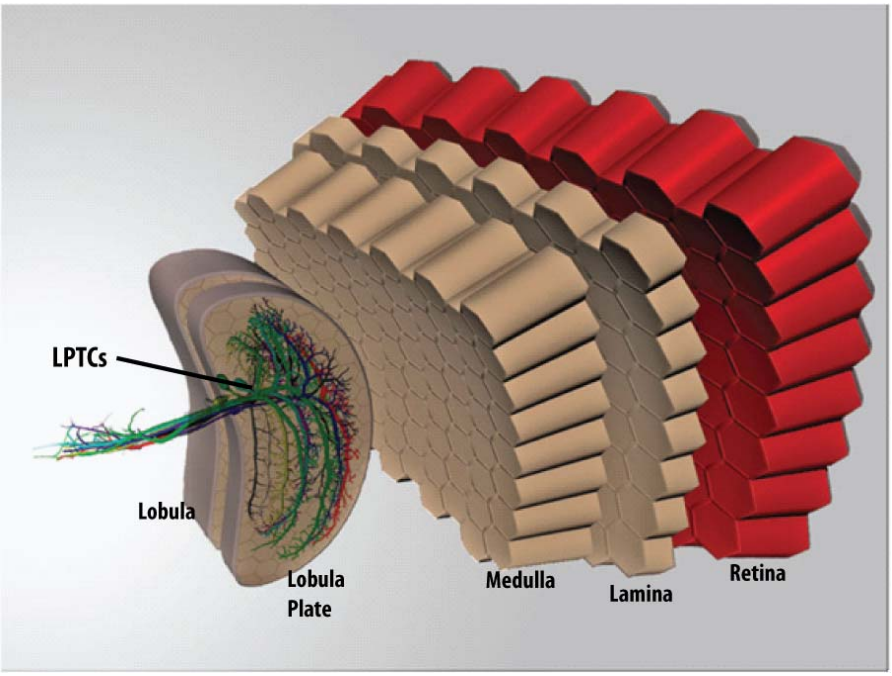

Figure 1: Spatial overview of the Optic lobe, with the vertical sensitive (VS) cells situated in the lobula plate. (Cuntz et al. 2007, A. Borst, 2010), added designations.

An optic lobe consists of three neuropiles the lamina, the medulla and the lobula complex, which is divided into the lobula and lobula plate. All these neuropiles constitute the same columnar structure as the retina - called retinoptry. Each of two chiasms, the outer one between the lamina and medulla and the inner one between the medulla and the lobula complex, reverses the image projection along the anterior-posterior axis (Braitenberg 1970; Borst et al., 2010). The cell body of all neurons within the optic lobes is situated in the cortex surrounding the ganglia, sending fibers into the neuropile, where they ramify and connect among each other. Lobula plate tangential cells, giant motion sensitive neurons cover the lobula plate. Descending dendrites finally lead to muscles, for example, those responsible for changing the present flight path(Wertz et al, 2008; Haag et al,2002,Haag et al., 2010).

2.3 Visual System of the Fly

A light beam enters the compound eye through the mosaic- like structure, the RETINA, composed of repetitive elements called facets or ommatidia.

Behind a lens, eight photoreceptor cells with underlying photopigment and supporting cells are always positioned in the same pattern within the facets. The photopigments are specialized for different spectral ranges (A. D. Briscoe and L. Chittka, 2001, Hardie,1979).

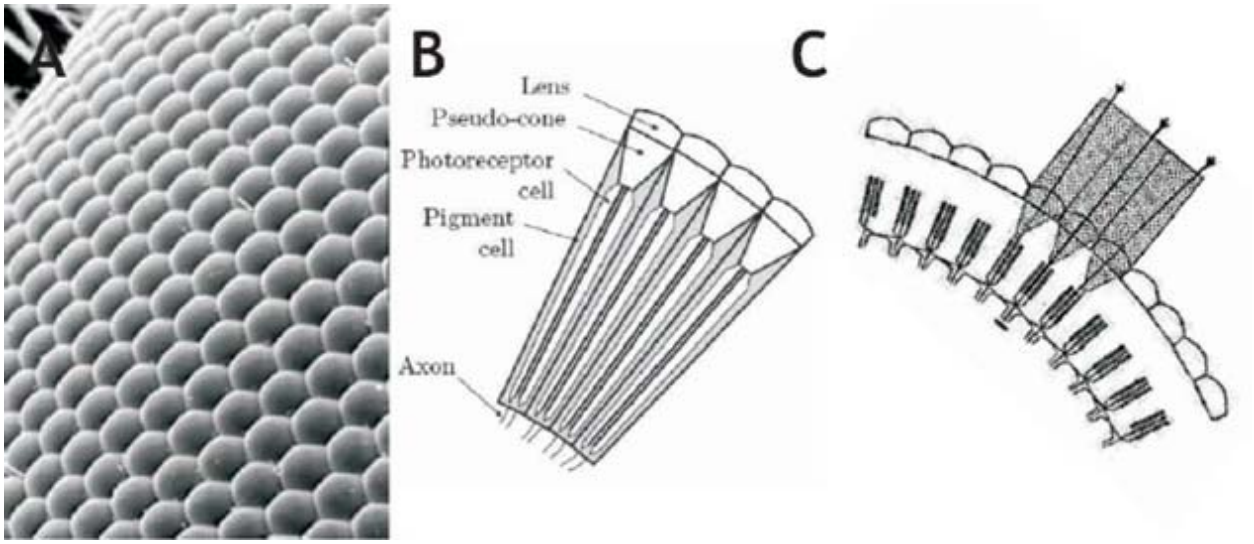

Figure 2: Retina (A) electron micrograph of the facet-eye of a blowfly (magnification of 375x) (from www.bath.ac.uk/ceos/Insects1. (B) the fly retina showing the basic structure of the light capturing device of a fly (Hardie, 1984). (C) Schematic of the neuronal superposition eye, in dipteran flies (Land(1997)), (adapted from M. Joesch, 2010)

They can be classified into two groups based on their morphology and the visual input for which they specialize. The outer group of the achromatic photoreceptors (R1-R6) is important for motion detection and contains wide rhabdomers, spanning the whole ommatidium (BorsZhu, et al.2009). They express Rhodopsin 1 and can be compared to vertebrate rod cells (C. Desphan. In the center of them, the inner photoreceptor R7 is placed on the top of R8, and occupies only half the space that the outer ones do. They are responsible for color vision in flies. Incoming photons cause a fast depolarization of the photoreceptors. Their potential can follow up to a flicker frequency of more than 300 Hz (Laughlin, 1999)

In Drosophila, each eye has approximately 750 ommatidia each with an internal angle of 4.6 degrees, distributed almost over 180 degrees. Imagine looking through the eyes of the fly and having a 500 fold lower spatial resolution than the human eye. The capacity of vision information is limited by the received input, and with enhancing the temporal resolution the

insects can compute visual input and perform their acrobatic maneuvers despite their coarse spatial resolution.

The achromatic pathway starts at the photoreceptor-monopolar synapses at R1 –R6 ending in the plexiform layer of the LAMINA, within retinoptic columns. These columns, i. e. the optic cartridges share photoreceptors with the same optical axis from six neighbored ommatida (I.A. Meinertshagen, 1971). This mechanism is called neuronal superposition and increases the sensitivity without scarifying acuity (Kirschfeld, 1973). Photoreceptor R7 and R8 pass the lamina alongside the cartridges and terminate deep in the medulla (Borst; 2010). Each set, including six photoreceptors, called visual sampling unit (VSU), ends presynaptic to a variety of interneurons. Five lamina monopolar cells, L1 –L5, two centrifugal cells C2 and C3, and the T1 cell, each embedded in every single cartridge, connect the lamina with the medulla (Borst; 2010). L2 supports L4, (Braitenberg, 1970, Strausfeld 1970) which in turn synapses via contacting two neighboring posterior cartridges back onto L2 (Braitenberg1970). Transmission electron microscope studies of the ultrastructure showed that L1-L3 and amacrine cells within the lamina receive direct input from R1 –R6 terminals via tetradic synapses (Meinertzhagen and O`Neil, 1991). L1 and L2, which are likely to be coupled via gap junctions receive their input from photoreceptors R1-R6.

The MEDULLA has as many columns as there are ommatidia of the compound eye. The lobula is composed of larger columnar cells, which are spaced one to every six medulla column, here a number of columnar cells were described (Fischbach and Dittrich, 1989). Many different input neurons branch in different layers of the medulla (Takemura et al. 2008) which is why it is thought to be a center for separating incoming signals in several functional pathways, such as detection of polarization, color or motion processing. Each medulla column houses in addition to the lamina cell terminals, many different columnar neurons, such as intrinsic medulla neuron (Mi), T2 and T3 as well as the transmedulla cells (Tm), connecting to the lobula, with transmedulla Y (TmY) cells additionally branching in the lobula plate. Columnar neurons receive only input from one ommatidium, whereas tangential neurons at the lobula plate receive information from several ommatidia.

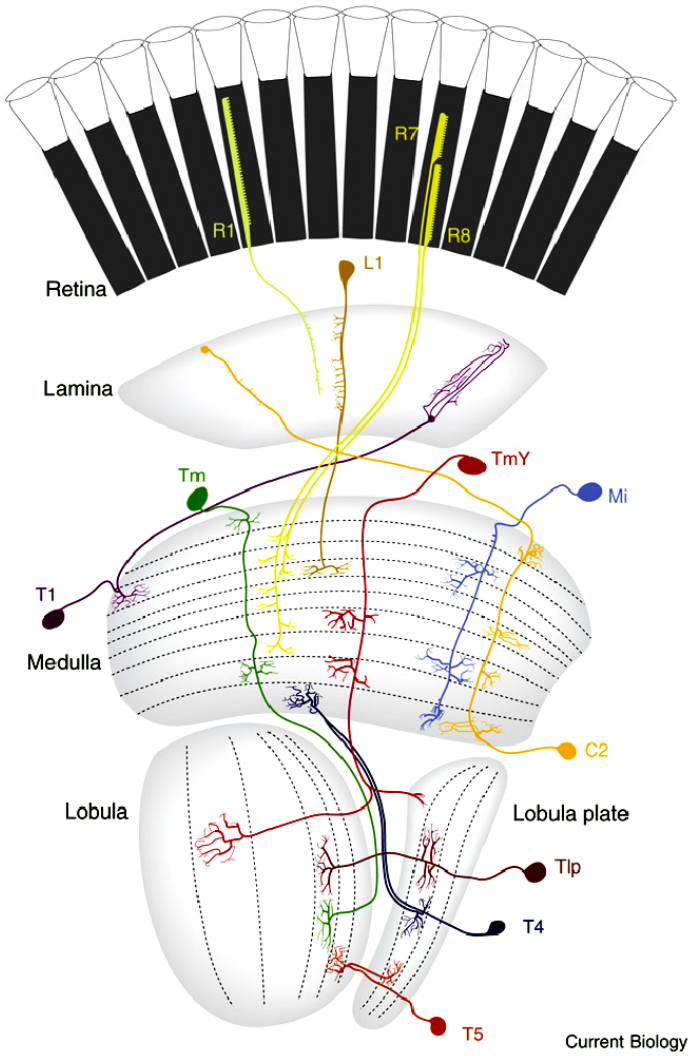

Figure 3: Columnar cell types in the fly visual ganglia. Illustration of typical neuronal connections in the fly`s optical lobe. Each single neuron represents only an example for one class of cell ((Borst 2009), modified after (Fischbach and Dittrich, 1989))

The previously mentioned Lamina cells are entry points to two parallel motion pathways, which were recently discovered to deal specifically with processing ON and OFF stimuli. One pathway starts from L1, which synapses onto medulla intrinsic neuron Mi1 which in turn is linked to T4 cells. Apart from that, L2 is connected onto transmedullar neuron Tm1 which is connected to the LOBULA, where it in turn contacts T5 cells. Bushy T4 cells connect the innermost layer of the medulla with the LOBULA PLATE. Furthermore, bushy T5 cells extend into the most posterior layer of the lobula as well as in the lobula plate. Both cell types are thought to play an important role in motion computations (Douglas and Strausfeld, 1996). T4 and T5 cells exist in four different subtypes (named T4a-d, T5a-d) per column and ramify in four different strata within the lobula plate, ordered according to direction. In Drosophila, the 2-deoxyglucose (2DG) method (Buchner et al. 1984; Bausenwein and Fischbach, 1992) proved the existence of these strata and that each becomes activated from a specific direction of motion. These different layers within the lobula plate are covered by appropriate LPTCs.

Named after their location and orientation, LOBULA PLATE TANGENTIAL CELLS (LPTCs) span large regions of the lobula plate tangentially, their axons go medially and end in the protocerebrum near the esophagus. Because the fly visual system is organized retinotopically, a fly`s visual surroundings are mapped onto the dendrites of horizontal sensitive (HS) and vertical sensitive (VS) cells, two types of LPTCs, by their connections to presynaptic columnar cells (Borst and Haag, 2002).

The morphology of VS cells and HS cells, of larger flies (Heisenberg et al., 1978; Fischbach and Dittrich, 1989, Scott et al.2002,) and recently in the fruit fly is well understood (Fischbach and Dittrich, 1989; Schnell et al.2010, Raghuet al. 2007, Joesch et al, 2008). These two types of giant output neurons reside face to face in a thin superficial layer of the lobula plate covering this region with their highly branched dendrites. Both VS cells, covering the posterior layer and the HS cells, covering the anterior layer have a direction defined preference within different parts of their visual field.

Drosophila has a network of at least six individually identifiable directionally selective cells, which cover vertical strata of the lobula plate with their overlapping dendritic fields (Joesch et al., 2008). The VS1 dendrite occupies the outermost region of the lobula plate and is followed in order by all other vertically sensitive dendrites. This type of LPTCs with lateral receptive fields become excited by downward motion (PD= preferred direction) in the center of their receptive fields and is inhibited by upward motion (ND = null direction) in the frontal part. These functions result in a depolarization or hyperpolarization of the membrane potential.

The dorsal (northern) HSN, the middle (equatorial) HSE and the ventral (southern) HSS cells are three individually identifiable cells electrically coupled within a complicated neuronal network. Tuned to large field horizontal motions in a directional-selective way, HS cells become excited by front-to-back motion on their ipsilateral side eliciting a depolarization. By motion in the opposite direction they are inhibited. Some tangential cells turned out to be sensitive to contralateral back-to-front motion, and thus respond to rotational panoramic motion stimuli.

2.4 Reichardt - Type Model

The direction of motion is not explicitly represented in the activity level of the photoreceptors. A model for elementary motion detection called Reichardt detector describes how a nondirectional signal is transformed into a directional selective signal at the level of LPTCs (Reichardt and Hassenstein). Motion vision represents a simple but well-defined example of neural computation. It is thought that motion–sensitive neurons with opposite preferred direction provide excitatory or inhibitory input to LPTC dendrites. Concerning the Reichardt model, these come in terms with the two mirror- symmetrical detector subunits. Each of them registers the luminance values (measured in two adjacent ommatidia) and after one is delayed it multiplies them by a low pass filter. In the last part of the model the resulting output signals become subtracted. The subtraction stage is realized on the dendrites of LPTCs (Borst and Egelhaaf, 1990, Joesch et al 2008). Due to the small size of the columnar elements in the medulla presynaptic to the LPTCs, the cellular implementation of the Reichardt detector is still not known.

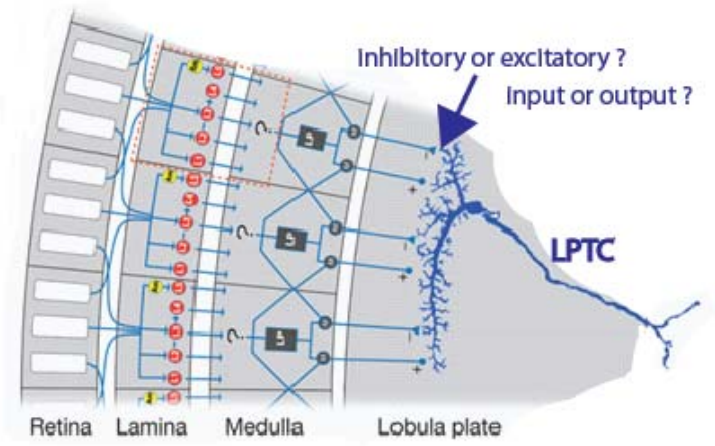

Figure 4: Reichardt detector, (M. Joesch, B. Schnell, 2010), modified

2.5 Meeting Point between Neurons - Synaptic Organization in the Fly

By looking closer into this system one can see how these neurons communicate with each other. At synapses, specialized cell- cell contacts, signals are transduced from a neuron to its target cell (R. G. Zhai and H. J. Bellen, 2004). Two fundamentally different types exist: Firstly,

electrical synapses occur at specialized sites called gap junctions. They form channels that allow ions to pass directly from the cytoplasm of one cell to the cytoplasm of the other. This transmission is very fast, thus, an action potential in the presynaptic neuron can produce almost instantaneously, an action potential in the postsynaptic neuron (S.H. Cardoso, 2001). A second way to communicate between cells is by chemical synapses. Electrical signals are converted into chemical signals that communicate between cells. Action potentials, arriving at the presynaptic terminal, cause calcium channels to open. Calcium ions diffuse into the cell and cause synaptic vesicles to release neurotransmitter, which then cross the synaptic cleft and bind to their distinct receptor sites at the postsynaptic membrane. This causes ion channels to open and transmitters diffuse into the cell, which in turn is able to produce an action potential. At the ultrastructural level it can be seen, that chemical synapses have a specialized structure. From the cytomatrix into the cytoplasm extends an electron dense projection where synaptic vesicles are tethered. Also at the postsynaptic site usually occur smaller electron densities. The synaptic cleft between the cells is wider than in electrical synapses. Both types of synapses are known to exist in the insect`s nervous system. The features and the basic architectural design are likely to be conserved among species (Palay, 1991; Zhai and Bellen, 2004). However, the high variability of tissues, neurons and molecular composition among different species may reveal a great number of ultrastructural uniqueness of synaptic sites.

Mammalian CNS synapses have pyramid-like dense projections. *D. melanogaster* is known to have also highly developed and characteristic appearances of synaptic compositions. So called T- bars, named after their typical T –shaped presynaptic electron density were found in photoreceptors, neuromuscular junctions (NMJs), and some central synapses (Prokop and Meinertzhagen, 2006). Adjacent to T- bars can occure electron dense bodies without such a typical shape. A study at NMJ terminals in crustacea has been proposed that synapses with prominent T bars have a stronger output, likely because more vesicles can tether and consequently release upon stimulation (Govind CK and Meiss DE, 1979; Govind CK et al., 2001). Within other fly species, such as the dragonfly the T-shape is much less obvious (Armett-Kibel et al., 1986) and was not found within ancestors of Diptera (Shaw and Meinerzhagen, 1986). In the adult brain of *Drosophila*, chemical synapses are in contrast to vertebrates generally not

found on the cell bodies (Prokop and Meinertzhagen, 2006). Neurons consist of an axon and dendritic extensions, which are located in the central neuropile, with the somata located in the outer cortical region. Another great difference of the insect`s synapses compared with

vertebrates is the abundant connection via multiple element clusters onto neurons (Lamparter et al., Meinertzhagen, 1984). As an exception to this, neurons at neuromuscular junctions were not found to form these assembles. In addition, even if various organelles which are involved in synaptic transmission are larger in the insects' nervous system, the overall size of the synaptic sites is generally smaller than in vertebrate counterparts (Meinerzhagen, 1993 and 1996).

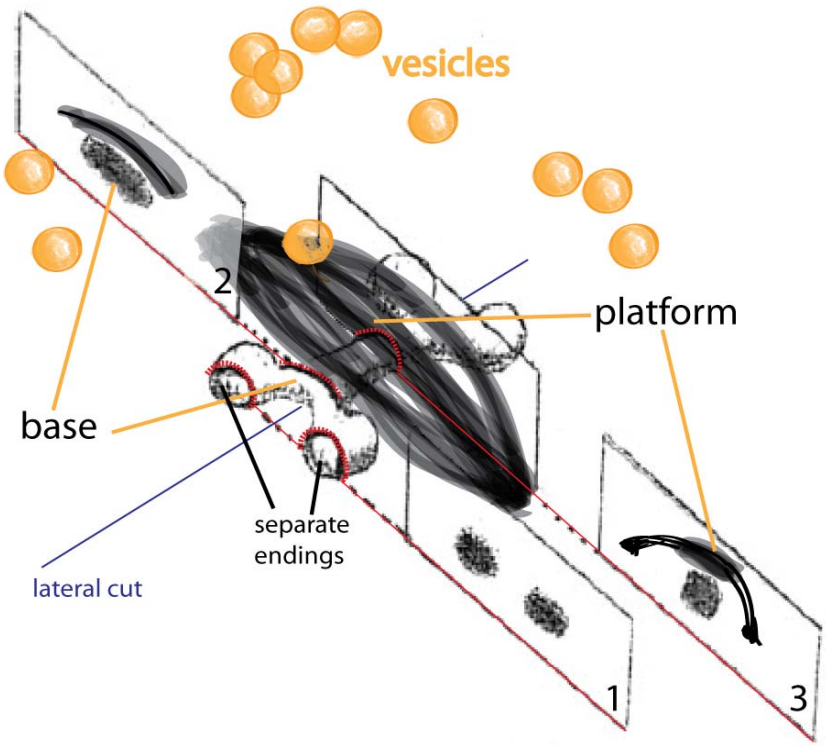

Figure 5: T bar projection, typically has a dense body bar and a platform on the topside. It is surrounded by synaptic vesicles. Depending on the plane of sectioning several shapes appear in cross-section (1, 2, 3), largest side would appear when laterally cut. (3D scheme adapted from J. H. Koenig and Kazuo Ikeda,1999, modified)

2.6 Neuroanatomical Studies and Application of TEM

Studies concerning motion vision in the fly began around in the end of the nineteenth century (Cajal;). Once started with behavioral observations, the first anatomical studies (y Cajal) up to more recent studies, with the help of physiological recordings and genetic investigations, achieved findlings of large field motion sensitive cells and the algorithmic model for elementary motion detection (Reichardt-detector) as part of computational research, raising hope that the course control network might be understood in the near future.

Each application serves as a piece of the puzzle ("visual driven behavior") and is a further step to its completition. Anatomical studies therefore serve as a fundamental research task which, further studies can build on. Since the late 1950s, the ultrastructural features of individual synapses were studied extensively, mainly by using electron microscopy. Resolutions obtained by light microscopy were insufficient, as dendritic and axonal processes can have diameters that are substantially below the diffraction limit of light. So far, only the electron microscope is able to resolve densely packed neighboring processes and neuronal geometry. Furthermore, it provides the spatial resolution which is needed to trace neuronal processes or to identify synapses unambiguously, which in turn can reveal the anatomy of connections between neurons within a complex neuronal system. Invented in 1932 by Ruska and Knoll, the transmission electron microscope (TEM) is the most used instrument in neuroscience for this purpose. A broad beam of electrons is directed at a sample thin enough to allow a substantial fraction of the electrons, which then project to an imaging device (e.g. fluorescence screen). Therefore the organism which is embedded into a plastic block has to be cut into thin slices. The result is an electron micrograph which provides a two dimensional cross section through that tissue.

Santiago Felipe Ramón y Cajal, said to be the father of neuroscience (A. Borst, 2010, talk) concluded the following more than 100 years ago about the visual system of insects, particularly about the compound eye of the fly: *"when one meditates, finally, on the infinite number and the exquisite adjustment of all these histological factors, so delicate that the highest powers of the microscope hardly bring them under observation, one is completely*

overwhelmed. And I, deceived by the unfortunate preconception of serial progress of zoological structures of similar function, hoped to find a very simple and easily studied architectural plan! It is indubitable that zoologists, anatomists, and psychologists have slighted the insects." (Santiago Ramón y Cajal, Recollections of My Life). Since that time, microscopes have gained greater spatial distribution and precision, thus revealing even smaller structures and successfully serving further functional applications.

2.7 Goal and Achievements

This study aims at expanding the current knowledge of the implementation of visual information processing in the fly brain. By having a closer look into the connectivity within the lobula plate, I investigate chemical synapses, highly specialized structures which facilitate the communication between cells. By using *Drosophila melanogaster* as a model organism, the specimens` brain is cut and prepared by EM- techniques, which enables its dissection with an ultracut- microtom. First, at the light microscope level, semi- thin sections (1µm) are analyzed to investigate an `atlas` of the flies` brain. This helps to orient within the optic lobes and also helps to the location of ulta- thin sections (70nm) of the lobula plate. Obtained ultra-thin sections are placed on a slotgrid, are stained and can finally be visualized by using a transmission electron microscope. Pictures at a magnification of 50,000X reveal a complex of cells which show electron dense profiles, specialized pre – and postsynaptic structures which can be analyzed according to their appearances of a dense body bars and further elements which indicate activity of synaptic transmission, such as vesicles associated with the presynaptic membrane, a widened synaptic cleft and postsynaptic profiles. A detailed analysis of synapses from a number of successive images provide insight into the ultrastructure of neuronal processes within the lobula plate and can serve for further classification studies of synaptic sites.

3 MATERIALS AND METHODS

3.1 SPECIMEN PREPARATION

SPECIMEN *Drosophila melanogaster* were taken from wildtype laboratory stocks (wt Berlin) bred under standard conditions. Adult females (distinguishable from their male counterparts by a brighter and distinct striped appearance of the abdomen, were selected from a population of sexes for further experiments) were chosen under carbon dioxide-induced paralysis and transferred to a beaker. After a short amount of time the flies regained a degree of motor functions and then each fly was subsequently immobilized by cooling on ice.

FIXATION Each fly was decapitated while held by its wings. The head was immediately transferred to a small basin filled with approximately 0.5 ml fixative within an agarose plate. The fixative was made of 2.5% Glutaraldehyde, 2.5% Paraformaldehyde, 0.2 M Cacodylate buffer and 7.2mM $CaCl_2$. A pH- value of 7.3 was adjusted and an osmolarity of 431mosm was determined. This plate was prepared with 10% agarose, made of 20g agarose and 200ml dd. water. Approximately a 1 cm x 1cm x 0.5 cm area was cut from this agarose within the plate using a scalpel and attention was paid to leave at least one nearly perpendicular edge. The focus of the binocular microscope had to be aligned during the immersion process. Using forceps, the fly was held by the proboscis and the head was cut in half along the eye, by using a micro-scissor (11`5 scissor).

The dissecting step for each of the final six specimens were done within three minutes and placed in different wells in a well plate filled with 1,5ml fixative. A loop made of a thin wire helped transferring the specimens into the wells. Adhesive forces held the specimens in the center without any contact to the material. Six plastic thimble-shaped tools with a net at the bottom were put in the fixative filled wells to push the fly head under the surface of the fluid as they would float to the surface of the solution, because of the air filled trachea and also the hydrophobic cuticula. Subsequently they were stored for 48h at 4°C enabling the fixative to

penetrate all intracellular structures. Three following wash cycles on a vibrating plate(75x), 10 minutes in fixative 0.1 M Cacodylate buffer, and 3.6 mM CaCl2 (pH 7.3, 217mOsm) secured the removal of all aldehyde substances.

POSTFIXATION Removing all residual aldehydes enables effective contrasting with osmium tetroxide, as remaining substances would interfere with osmium tetroxide. The samples were postfixed for one hour in a solution consisting of 2% osmium tetroxide solution, buffered with 0.1 M Cacodylate buffer containing 2.25% sucrose and 3.6 mM $CaCl_2$ at room temperature. Afterwards the brains were washed with 2 ml of 0.05 M Cacodylate buffer. The incubation with osmium tetroxide fixes all (membrane) lipids in the preparation, visible as electron material of all membranes afterwards in the electron microscope. Afterwards the specimens were washed with 1:4 diluted 0.2 M Cacodylate buffer and 7.2mM $CaCl_2$ and 4.5% sucrose.

DEHYDRATION Each step of the following graded dehydration took 10 minutes on the rotation wheel. The graded increasing ethanol series of two times 30% , 50%, 70%, 90%, 95% (old 100%) was completed by transferring the brains twice into 100% ethanol for 15 min each.

TRANSITIONAL SOLVENT INFILTRATION Propylene oxide was added two times for five minutes each and served as a hydrophobic carrier substance. These steps require a remaining fluid around the tissues to avoid a desiccation.

RESIN INFILTRATION Pure Epon, a hard plastic material tolerates the pressure of cutting and was used to embed the tissues. Epon was made of 10 ml Glycidether (resin) with 6 ml of Methyl nadic anhydride (MNA) as well as 4.5 ml of Dodecenyl succinic anhydride (DDSA) and the accelerator 0.6 ml Benzyl dimethylamine (BDMA). The brains were transferred to the listed mixtures of Epon with Propylenoxid ensuring a gradually and sequentially penetration of the resin.

1:2	Epon : Propylenoxid	for 0.5 h
1:1	Epon : Propylenoxid	for 1h
2:1	Epon : Propylenoxid	for 0.5 h

The lid was opened over night, in order to evaporate the propylenoxide.

EMBEDDING The brains were mounted in a sagittal orientation with the eyes into the tip of embedding molds. The polymerization needed minimally 48 h at 60 C to cure in the oven.

TRIMMING While watching under a stereomicroscope (Leica MZ6) the Leica EM TRIM2 milling maschine was used to trim the blocks from three edges around the specimen with a set angle of 45 degrees. This pyramid-like block terminal had symmetrical sides of 800µm and one less trimmed side of 1000 µm.

3. 2 Semi Thin Sectioning – The "Atlas of the Optic Lobes"

Sections of each 1 µm were obtained in the ultramicrotome Ultracut E (Reichert Jung) and immediately transferred from the water basin into a culture dish with methyl blue. The dye was placed on a hot plate to avoid a destruction of the tissue. After washing, the sections were transferred with a wire loop to an object slide. These semi- thin sections were produced to give a first insight and overview of the organization and section plane of the fly. As previously mentioned the brain was opened by cutting it in half along the left eye. Thus the fixation of the central brain and the opposite eye was ensured. For a better understanding of the overall dimensions see the three-dimensional fly head looking into the paper. The "drosophila atlas of the optic lobes" of block no.C79_2 facilitated the later identification and orientation within the optical lobes to start ultra thin sectioning. Through this, the starting position and the end of a representative insight of lobula plate were noted (64 µm and 91µm). By using a confocal light microscope images were taken of the semi thin sections from the first slice of the optic lobe to the end of it. The pictures were rotated and aligned with Image J to be uniformly orientated. At block C79_3 the Epon was shaved off in 1µm increments to a depth of approximately 60µm, the first cut of the lobula plate. It was known that a removal of up to around 60 slices is possible

before cutting the lobula complex. Thus, not every section was processed in the same way as the “atlas” before to look into more details.

However, to ensure quality and the right position, 56 sections were captured and stained to help orientate within the object. As progress was made deeper into the lobula plate, a shorter distance between steps was chosen. The current position had nearly the same section plane as on the pre-created sagittal optic lobe atlas. As the lobula plate was reached, two more semi-thin slices were cut and the block was prepared for ultra thin sectioning.

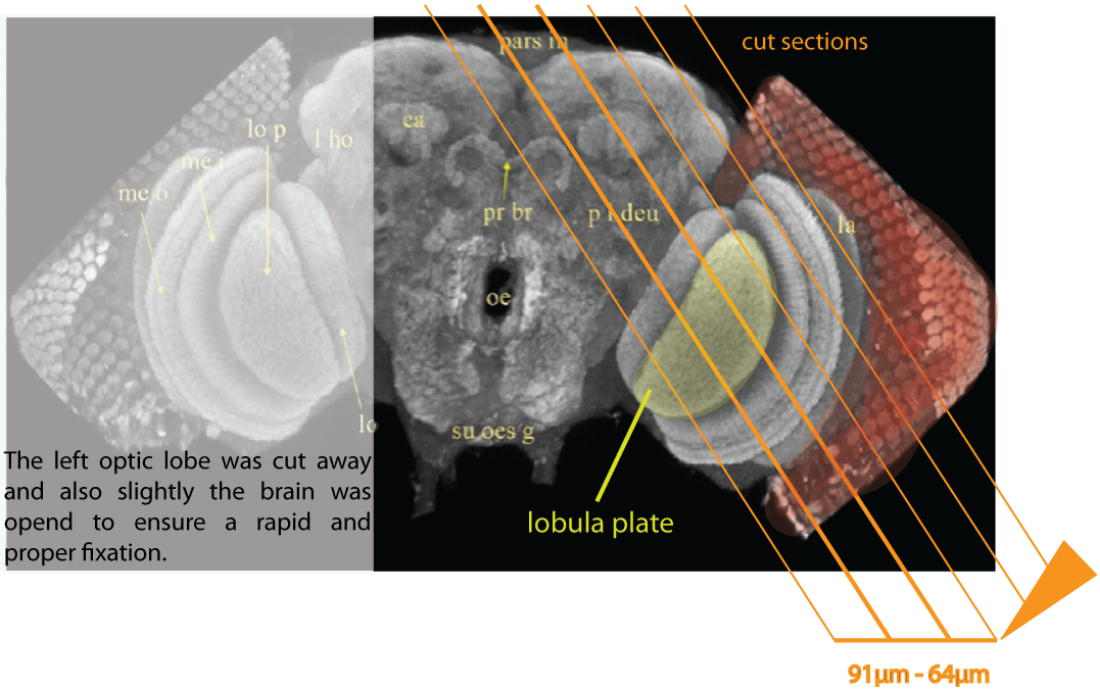

Scheme 1: The head of *Drosophila* from behind reveals the two optic lobes. Outline of the cutting and dissection steps. The picture is modified and was taken from the `flybrain` webpage, Dalhousie University.

3.3 Ultra Thin Sectioning

For ultra thin sectioning the pyramid was trimmed with the 45 cryotrim knife (CT795) from Diatome, fixed in the ultra microtome. The whole brain cross- section fit into a rectangle of 250 x 350µm. The final rectangular face of 150 x 100 µm included the lobula plate at the

lower end, surrounded by its neighboring lobes. The depth that the trimmer needs to run at was determined and measured at the semi thin sections.

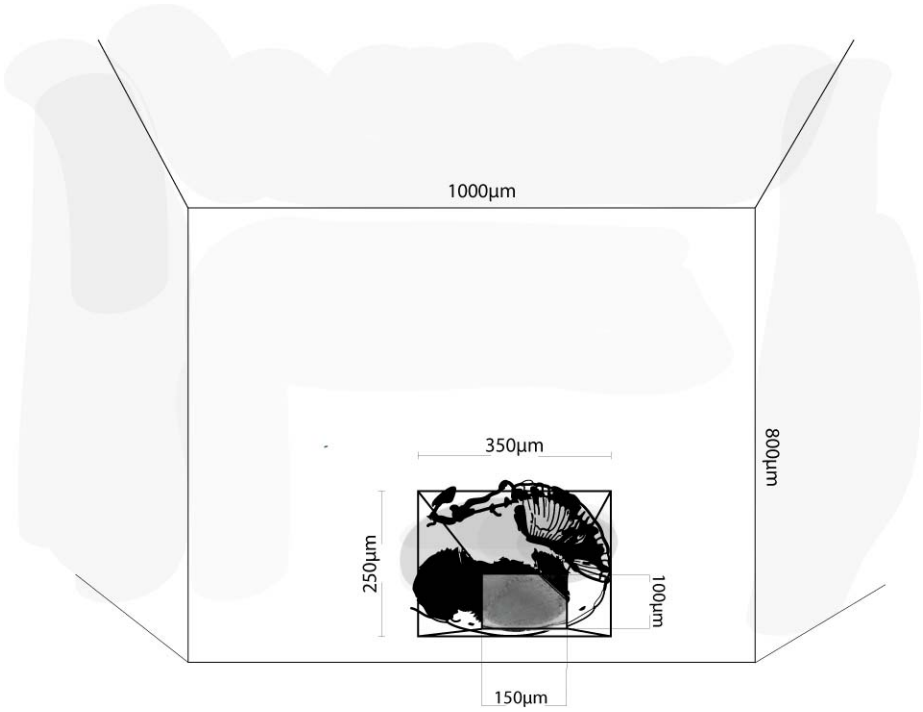

Scheme 2: Epon- block with embedded fly brain. A second smaller pyramid-like shape was trimmed to receive smaller sections. A face of approximately 150µm x 100µm was obtained. The front of this truncated pyramid shows the area from which the semi- thin images were taken from. The underlying remaining fly brain is depicted as a black scheme.

The right upper corner was removed at a 45 degree angle, serving to separate the ribbons of later sections when floating on the surface of the water. In addition, one can later orient and ensure the right position on the slotgrid. Using a DuPont diamond knife the cutting was started in the region of the lobula plate, examined from the semi- thin sections. These sections removed 2 µm from the block. It was necessary to trim additional microns with the Diatom cryotrim 45 (CT795) to maintain a face with the same size and shape as before. To yield the optimal force distribution during the cutting process it is recommend to position the longer side upright and perpendicular to the knife edge (C. Kapfer, personal communication). No angles were set at the adjustable devices of the ultramicrotome. The velocity of the automatic mode was 1 to 2 mm/s. A yielded section thickness of 70 nm has a silver grey interface color. Just before sectioning the slotgrids were coated with a polioform membrane made from a 0.75% polioform solution (with chloroform). These prepared slotgrids held with forceps were dipped into the water-filled knife container and lifted through the water surface to optimally capture a

ribbon of three slices each. Other colors like gold indicate thicker sections of about 90 nm. Purple or blue sections were discarded because they are too thick. Hydrophobic properties of the water made it difficult to place the ribbons exactly in the middle of the slotgrid. A lash was used for handling and gating these sensitive structures. Professionals know revealing a complete serial section of a stack takes a great deal of training; from several months to years. In this study it was feasible to take two of the fly brain blocks and practice for several days. Thus some of the final sections of probe C79_3 did not properly fit to the film on the slotgrid or the ribbon became separated during the lifting process. Another disturbance in serial sectioning occurred when slices stuck to the lash while turning the ribbon. The knowledge to perform this work mainly came from different movie clips (Harrison) and a technical assistant. After air drying sometimes with the help of filter paper, each slotgrid was transferred into a slotgrid storage box with a given number of the position.

30 slotgrids were selected and placed into a holding device for staining. The entire automatically staining process in the Leica Stainer (Typ 2168-002) with uranylactate lasted 20min at 30°C and with lead 1 min 20sec at 20°C, respectively. Each was then stored back to the slotgrid box for later photographing in a transmission electron microscope (TEM).

3.4 Transmission Electron Microscopy

Using the Transmission Microscope (JOEL JEM1230HC; 50000X), images were taken of the contrasted ribbons. It is preferred to obtain a perfectly uniform section thickness which exhibits no folding. Firstly the sections were analyzed directly on the transmission electron fluorescent screen. By scanning through the sections, the orientation was discerned by the removed right edge along with the axon bundle which runs through all slices in the middle of the lower end of the slice. Then a position nearby the axon bundle was searched with a few nanometers below the cell bodies surrounding the lobula plate. After obtaining an overview at a 5000X magnification proper cells were selected at a magnification of 50,000X. Tangentials which were relatively large in diameter were preferred to trace at, this raises the probability for more

including synaptic sites. When successfully found a suitable tangential (approximately 1µm) the first image was taken. Sometimes an extra image was taken at 10.000X to orient within the tissue and to estimate the distance to landmarked structures. The highest magnification which was used reveals an image which represents the ultrastructure of a single cell in a detailed resolution and provides enough detail to see cell compartments such as mitochondria, membranes, small vesicles, up to tiny synapses and even coarse shapes of participating proteins. From the images taken at a higher magnification, a neuron was difficult to find on the following section. Characteristic landmarks, help at which one can orientate. The search for the same cell on the next slice takes time. It is important to be totally sure to observe the right traced structure otherwise lacks scientific evidence.

Slotgrids from the slotgrid storage box at the position D2, E2, G2, G4, J1, J3, J4, K2, L4 and L5 were studied. Construction works avoided a further use of the device and thus slotgrid M1, M2 and M3 were studied under the TEM FEI MORGANI. This TEM has a lower resolution and did not reveal representative successive sections and thus analysis using this device will not be explained in any further detail. Most of the slotgrids contained 3 slices. Despite the attention to the right side of the slotgrid, while operating the TEM it is difficult to identify the order of the slotgrids. Thus, in case of uncertainty an image was simply taken and that the order could be determined later on.

3.5 EDITING IMAGES

The semi thin stack was converted into 8 bit images, filtered with a Gaussian blur filter of 0.6 Ω and the contrast was aligned and finally registered with the Image Analyzing Software Fiji Linear stack alignment with SIFT, which has a high maximal alignment error of 70.00 pixel. The traced head capsule was cut from the surrounding outline of Epon matter. Afterwards the image was turned, thus that the right compound eye is laying right lateral and the optic lobe posterior. The central brain lies in a higher level. After adding the scale bar the images were saved sequentially. 3D -stack exposing the compartments of the optic lobe and the final location within it was processed in Amira 5.3.3 and finally edited in Adobe Illustrator.

The ultra thin stacks were converted into 8bit image size, the Gaussian filter of 0.8 Ω for the picture taken with the JOEL- TEM. They were ordered into single stacks to match the successive following slices. By appropriating distinct layers and lowering the opacity of the underlying one in Adobe Photoshop the images were aligned. The images were packed into single folders including the stacks of successive images, upon which an evaluation followed. The further analyzed and described images were sections from slotgrid J1, J3 and J4. The images from the last two mentioned slotgrids had to be numbered the other way around. The reasons for this selection were at the one hand the better quality from higher resolution in the Joel- TEM, where the mentioned slotgrids were investigated.

3.6 Analyses of the Ultrastructure

The analyses of the two stacks supposed to reveal synaptic ultrastructure within the lobula plate was done by the help of the Image analysis Software (Fiji). The area which included the traced neuron terminal was cropped as an image sequence and a scale bar was added. All analyzed sections were revealed at the magnification of 50.000X. The diameter, perimeter of the traced terminals, amount, size and types of synapses as well as diameter of synaptic vesicles, which are thought to participate in synaptic transmission (surround the presynaptic electron dense body in a distance of maximal 50nm), either docked at the presynaptic body or surrounding it. In the (Scheme 3) the exact determinations for the measurements on synapses (especially T- bars) are delineated. The detailed measurements are listed in attached tables and illustrated by explaining representative examples.

Analysis criteria for synapses: presence of a number of synaptic vesicles associated with the presynaptic membrane, a widened synaptic cleft, the presence of a dense body bar or T- bar and postsynaptic density with possible specializations. The average value from the single values of height and width of the dense body as well as of the values of matrix is calculated per synapse. Then the average of these averages is calculated and noted as total value. The average of the maximum platform per synapse and all the average of all noted diameters of the vesicles

are calculated. The average values with standard deviation show the mean and the corresponding significance of the measured values.

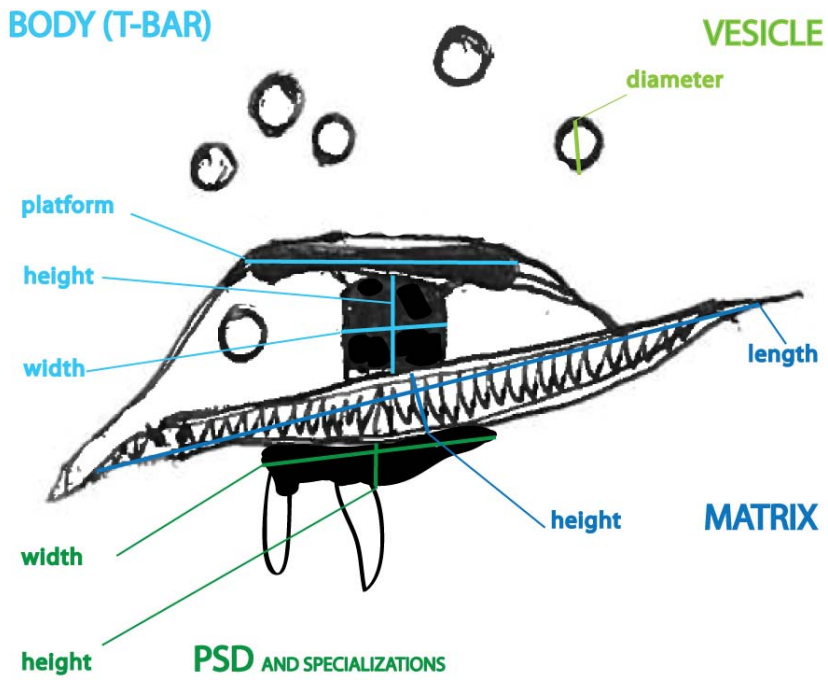

Scheme 3: This scheme shows the determined measurements on synaptic sites.

- body
- vesicles
- postsynaptic density (PSD) and specializations
- matrix

Counts of synaptic profiles in single sections are necessary when studying serial sections. Only the examination of the corresponding profiles in sections lying on either side in the series make it possible to confirm which profiles were those of synapses.

4 RESULTS

4.1 Semi Thin Sections – – The "Atlas of the Optic Lobes"

This stack of sections is a run through of the optic lobe of the fruit fly, starting from a cut through the retina and anterior medulla to the last optic lobe, the lobula complex. The head capsule is 250µm in height and 350µm in width. The first images reveal a typical cross-section of the eight characteristically arranged photoreceptors within ommatidia. This is easy to recognize within the red colored retina.

Each slice is cut at 1µm. A stack of about 31 µm sections was sagittaly removed from the eye until the redundant, the lamina, was seen. The optic lobe is situated behind the retina within a distance of 33µm. From this point on the sections were recorded with the camera mounted in the light microscope (LM). The total stack of the optic lobe, including non -photographed and immediately removed slices has a range of approximately 78µm. Sections which showed folded tissues were noted but not integrated into the optic lobe atlas, because no information could be obtained of them. A range of 67 sections through the optic lobe were photographed. Finally a stack of 56 slices was selected and aligned.

The lenses are the entrance to these columns, seen as semicircular arrangement around the eye. On the first section one sees the first part of the optic lobe the lamina, posterior to the cluster of connecting photoreceptors. The second image shows the cortex of the second optic lobe, the medulla. Within a depth of 37µm (image 4 and 5) the first (outer) optic chiasm, reveals connecting axons. The first slice of the medulla cells under its surrounding cortex are visible at a depth of 41µm (image 8) directly behind the lamina. Large dark regions indicate stained sheets of glia cells around the optic lobes. Cell bodies of monopolar lamina cells reside as groups above the optic cartridges, between the lamina and the basement membrane of the retina. The sagittal sections cut the lobes obliquely, such that the optic cartridges can be seen. Dorsal to the optic compartments one sees the lateral margin of the lateral horn which belongs to the protocerebrum. This is the most lateral part of the superior lateral protocerebrum.

At a depth of 60µm (Image 23) the two medullar layers, an outer two third and an inner third can be seen. At this depth the lobula complex can be seen, composed of posterior lobula plate and the anterior lobula. Between this complex and medulla the second optic chiasm can be seen. Within the medulla exist several layers, such as the bright one appearing in the middle of this optic lobe. Further proximal the inner medulla starts. The retinoptical organization, which occurs in all optic lobe neuropiles is especially obvious within the lamina and outer medulla. In slice 36, at a depth of 72 µm crossing the middle of the medulla, nicely exposes a cross- section through all compartments of the optic lobes (*Figure 1*). The organization of the columnar projection in the lobula complex is rotated at an angle of 90 degrees. Here, the brain above already has the volume as the optic lobe. Within the last sections (54) at a depth of approximately 93µm, the last part of the lamina Cuccatti's bundle can be seen, and contains the axons of medulla and lamina tangential neurons which enter the posterior optic tract. The last depicted sections showed the medulla and the lobula complex. Behind retina and lamina appear muscles which control the antennae and mouth. The very end of the lobula complex was reached at a depth of 105 µm, thus the lobula plate was found to span a depth of 60 µm to 105 µm. Thin- sectioning in different specimens was set to start in a depth of 64 µm, where the greatest volume of the lobula plate is seen.

Figure 1: **From semi thin to ultra thin sections**, through the optic lobes of the fly conveyed to the ultra thin sections within the lobula plate. The overview was investigated to enable a dissection of ultra thin slices at the right position in the lobula plate.

From semi thin to ultra thin sections

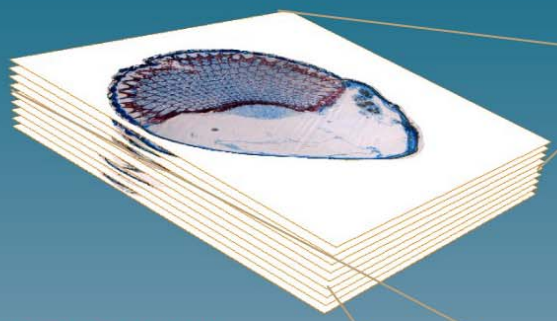

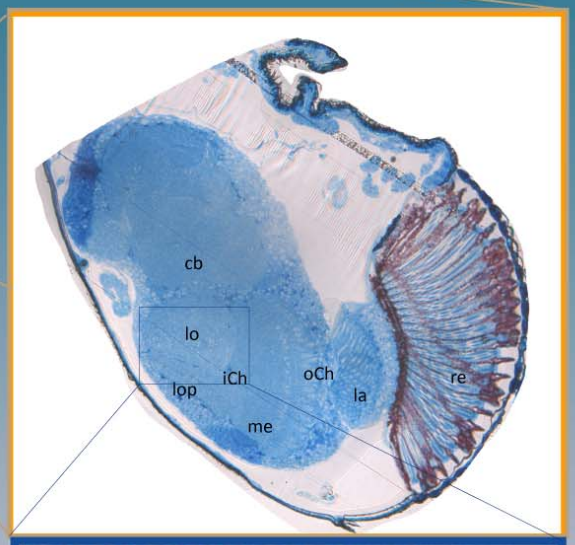

The final aligned stack of 56 images cut saggital through the optic lobes of *Drosophila melanogaster*. Slice 36: An extract from a depth of 72 µm reveals all compartements of the visual pathway. Proximal to the arrangement of photoreceptors within the retina (re), the lamina (la) shows its coloumnar structure. The latter is connected via the outer optic Chiasm (oCh) turning the columns around its vertical axis, but preserving the order in the second optic chiasm, the medulla (me). The smaller part of this layer, the inner medulla attached to the lobula complex, composed of the lobula (lo) and the lobula plate (lop) via the inner optic Chiasm (iCh). In the surrounding position cell bodies housing cell bodies of coloumnar cells and separate the optic lobe from the superior central brain (cb).
Magnification: 40x

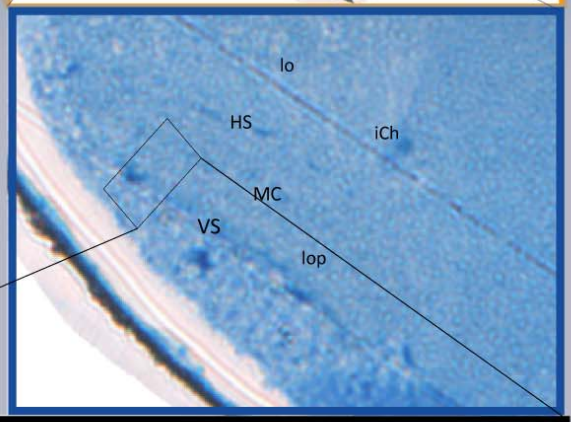

The close-up pf the lobula plate thightly shows three planes of the dendritic branches of LPTCs:
The vertical sensitive (HS) cells at the superfical layer of the LP attached to the surounding cortex. The horizontal sensitive (HS) cells at the opposite side reside in the neighborhood of the lobula.
In the middle is a so far not described cell type (MC).

TEM picture: lobula plate.
Scale bar: 5µm

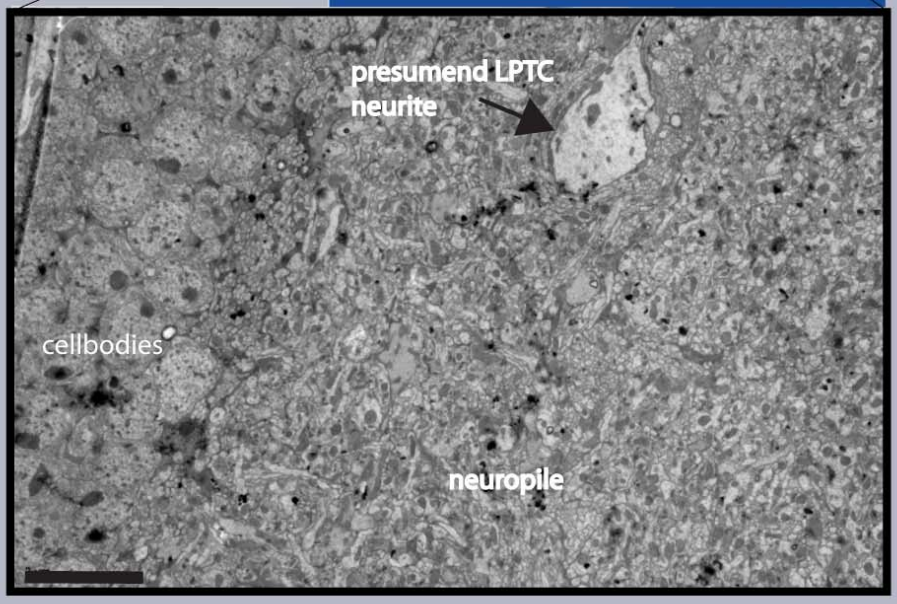

4.2 Ultra Thin Sections –Ultrastructure within the Lobula Plate

4.2.1 Overview

All of the obtained pictures are presumably exposures of terminating columnar neuronal cells and tangential neurons within the lobula plate (Figure 1). Because the left eye was sagittally removed, columnar cells are seen laterally cut. In contrast, tangential cells positioned perpendicular and thus, they can be seen in cross-section.

This study investigated the organization and ultrastructure of chemical synapses, presumably on tangential cells within the lobula plate. We focus on possible structural differences among synaptic connections to figure out, if structural features may be indicator for known functional implementation onto LTCPs. The central part of the lobula plate is visualized, where LPTCs are known to run through this area.

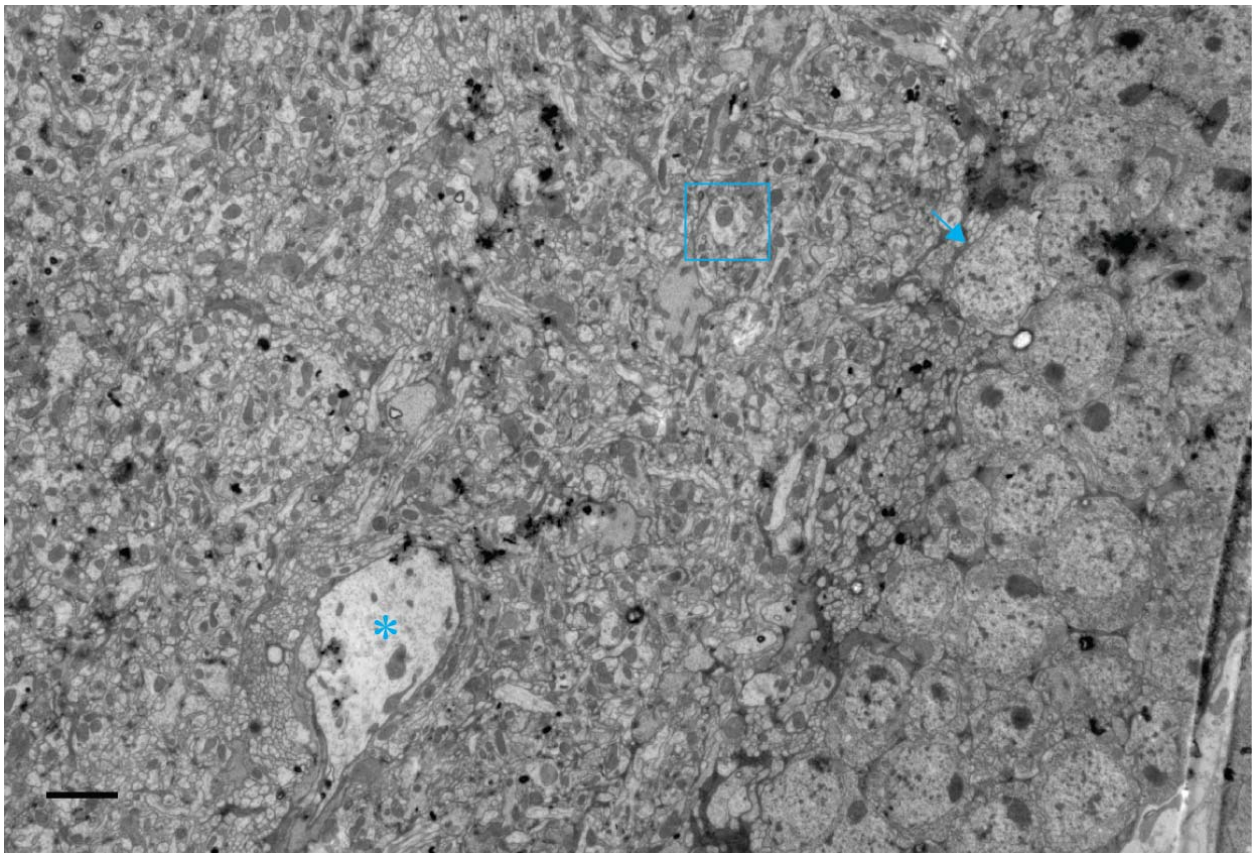

Figure 2: **Exposure of the lobula plate (1),** at a magnification of 5000X. From the cell (square), three images at a magnification of 50.000X were taken, shown in Figure 4. This overview is necessary to find the same cell on the next section on the slotgrid. The characteristic cell bodies (arrow) at the edge of the brain and the neurite (asterisk) served as landmarks. The latter belongs to the axon bundle of the LPTCs, which converge at distinct point within the lobula plate. Scale bar 2µm.

The two analyzed stacks presumably show tangential cells which run relatively close to each other, approximately 6µm apart (Figure 2 and Figure 3). Seen on the left side of both of the stacks are the cell bodies surrounding a part of the lobula plate. 90 degrees and 6µm from the cell bodies, relatively bright cells (blue, Figure 2) can be seen. The higher magnification revealed ten synaptic connections from the first series of three images and seven synaptic connections from the second stack of five. Great attention was paid to the ultrastructure of chemical synaptic sites, consisting of a presynaptic electron density (dense body) and a postsynaptic electron density (PSD).

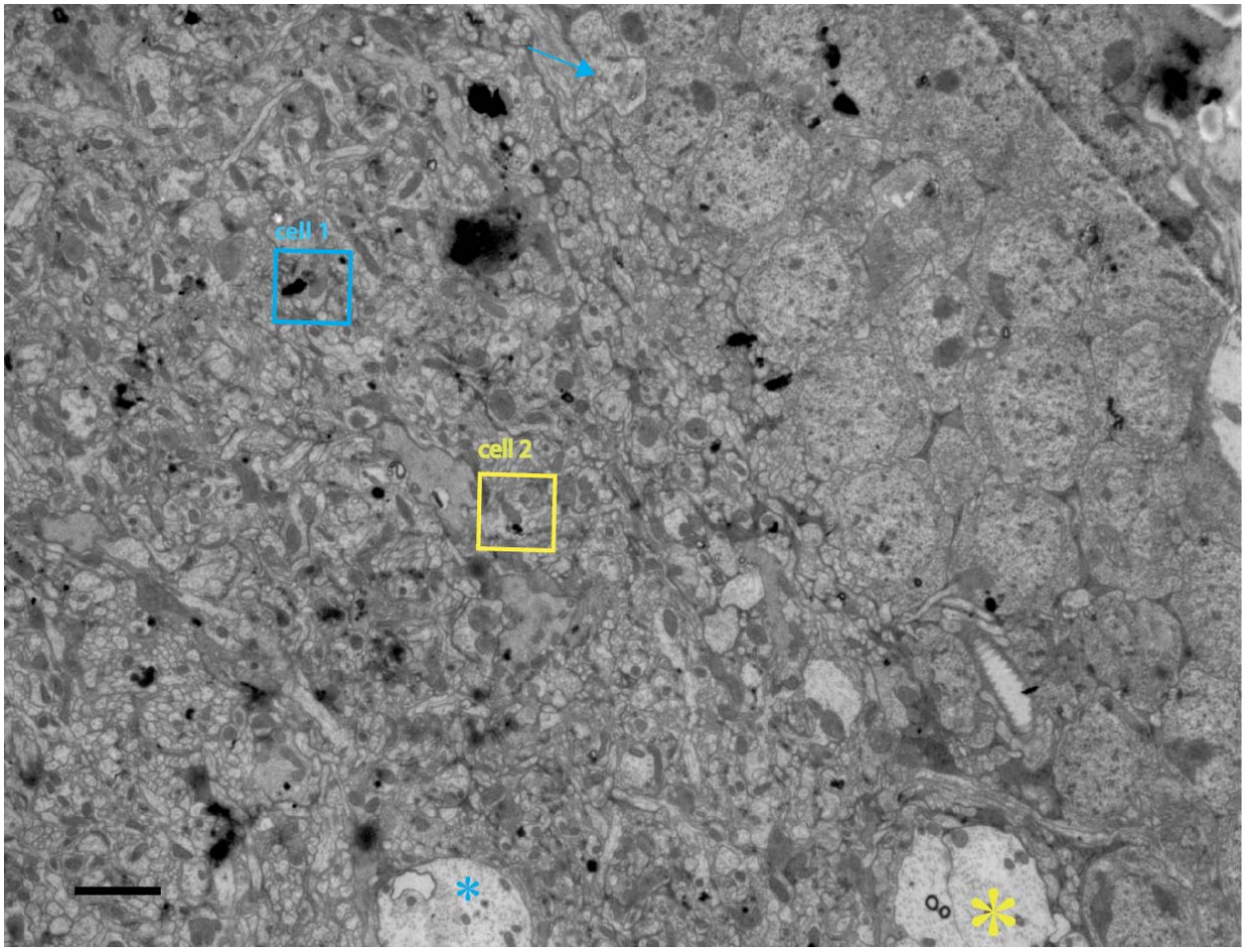

Figure 3: **Exposure of the lobula plate (2),** at a magnification of 5.000X. Approximately 630nm (9 sections) deeper situated in the lobula plate, than the first overview showed. The cell (yellow square) is the last of five images which were traced at a magnification of 50.000X. Beside these cells, run presumably two converging axons which also served as point of orientation. The above now shows a part of the axon bundle (yellow asterisk) in the lower right corner and again the axon (blue asterisk, also in Figure 2). The characteristic cell bodies (arrow) served as a landmark from the first stack, thus the first cell (blue square), which has changed shape from the previous image. In higher magnification, cell 1 can be seen in Figure 4 and cell 2 is shown in Figure 5. Scale bar 2µm.

STACK 1

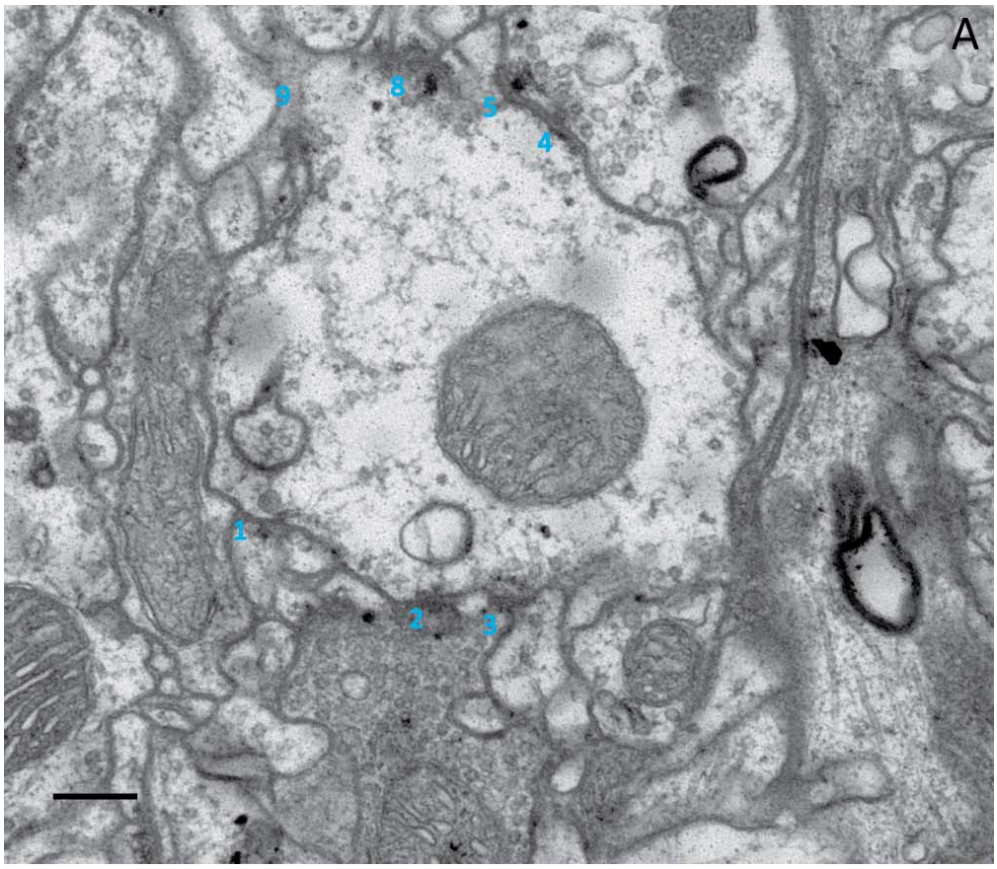

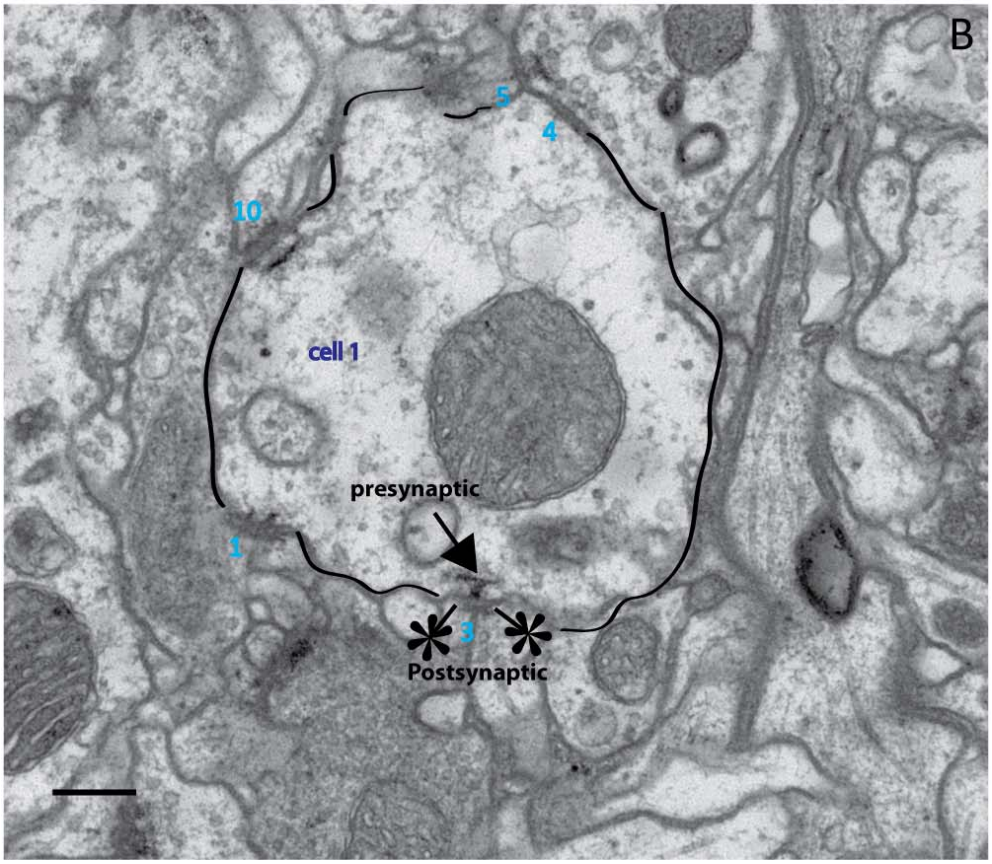

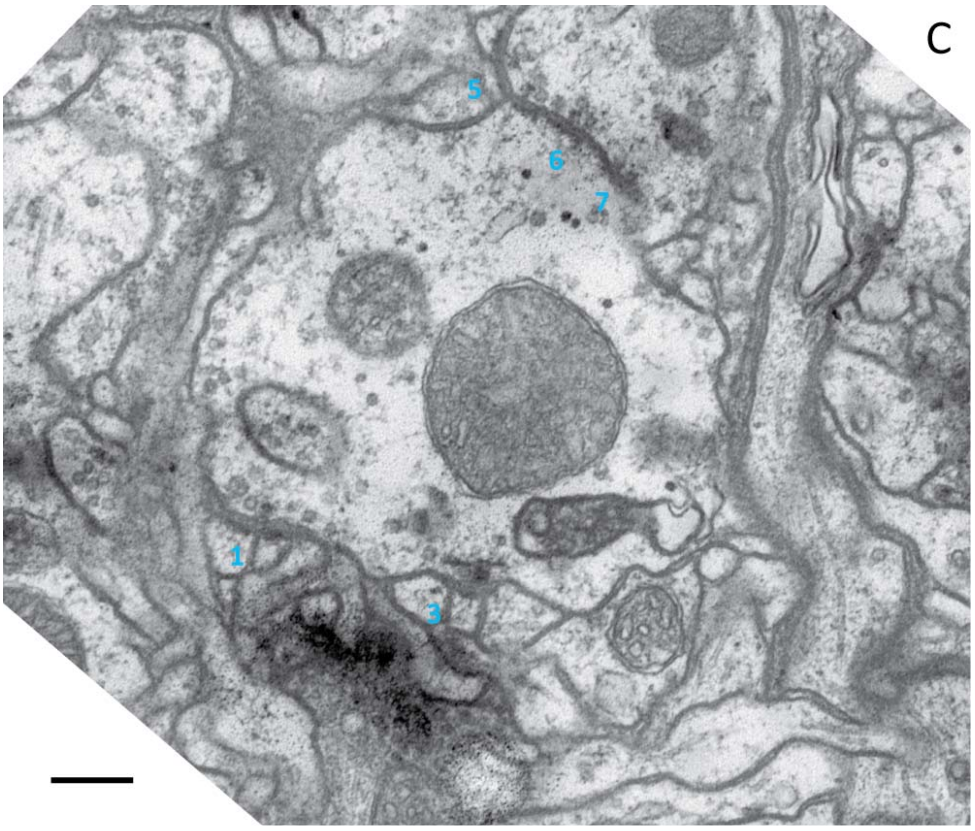

Figure 4: Stack 1 consists of three successive aligned images. The nearly round cell in the center was analyzed (marked in B), has a perimeter of averagely 4.7(±0.2)µm(n=3), covers an area of 1.3(±0.1)µm^2(n=3) and has a depth of 210nm (n=3). A synaptic site (arrows in B) can be identified from the high electron density separated into the presynaptic input site along with the postsynaptic density (PSD) at the opposite output site. The cell is surrounded by a number of maximal 19 cells, 12 of them connect to the investigated tangential cell. All identified synapses were numbered and listed consecutively with corresponding features in table 1. Magnification of 50.000X, scale bar 0.2µm.

The synaptic sites (synapse), in this study, were classified according to type, number of connections, size, location, if on the pre- (defined as output) or post- (defined as input) side of the cell, number and size of vesicles, which surround the cell in a distance of maximal 150nm, and length and height of the widened matrix. Additionally, the postsynaptic densities were classified according to their shape. Among the two investigated cells visible in eight different sections, a total of 17 synaptic connections were identified and closely studied. All synaptic connections were highlighted with a number. Those in table 1 correspond to stack 1 and those in table 2 correspond to stack 2. Following representative close-up stacks are explained into more detail within the results. The number of these close-ups is determined by:(no.**x** (no. stack).**y**(no. synapse)).

STACK 2

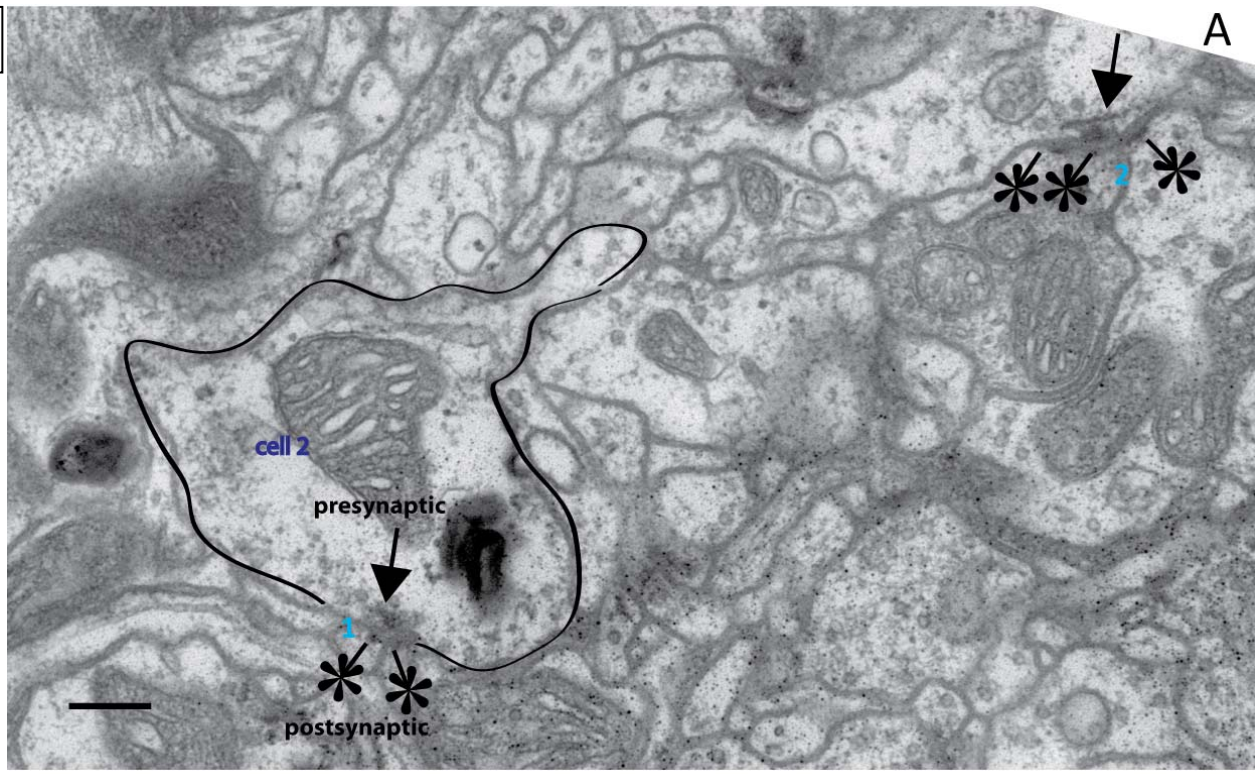

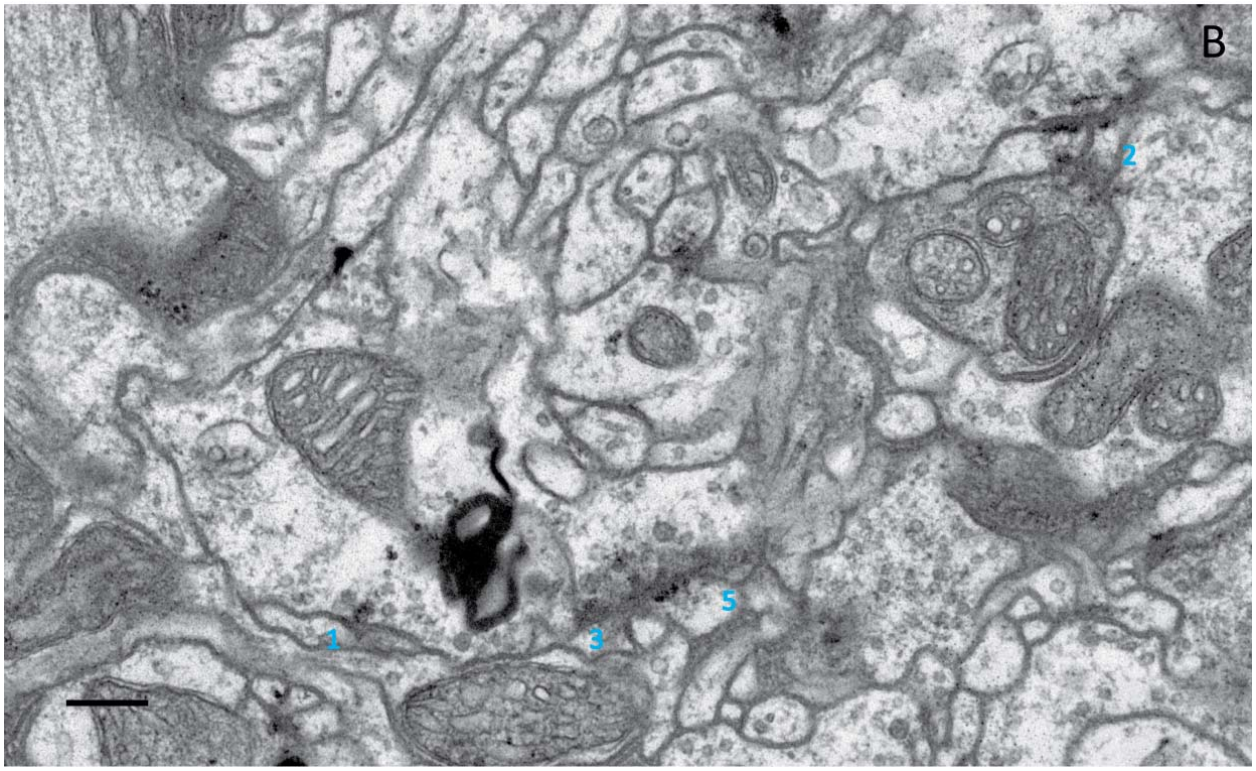

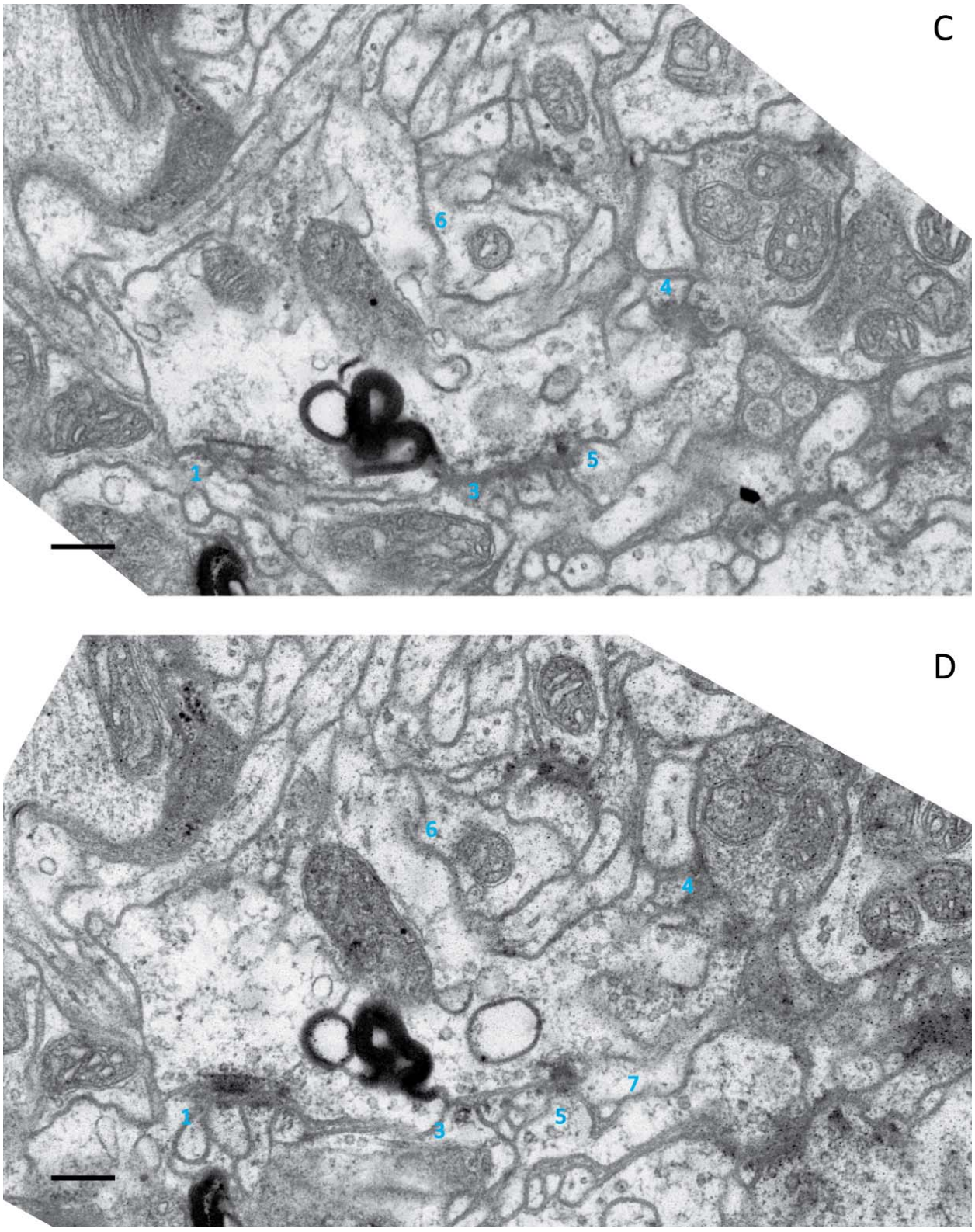
C
6
4
5
1
3
D
6
4
7
1
3
5

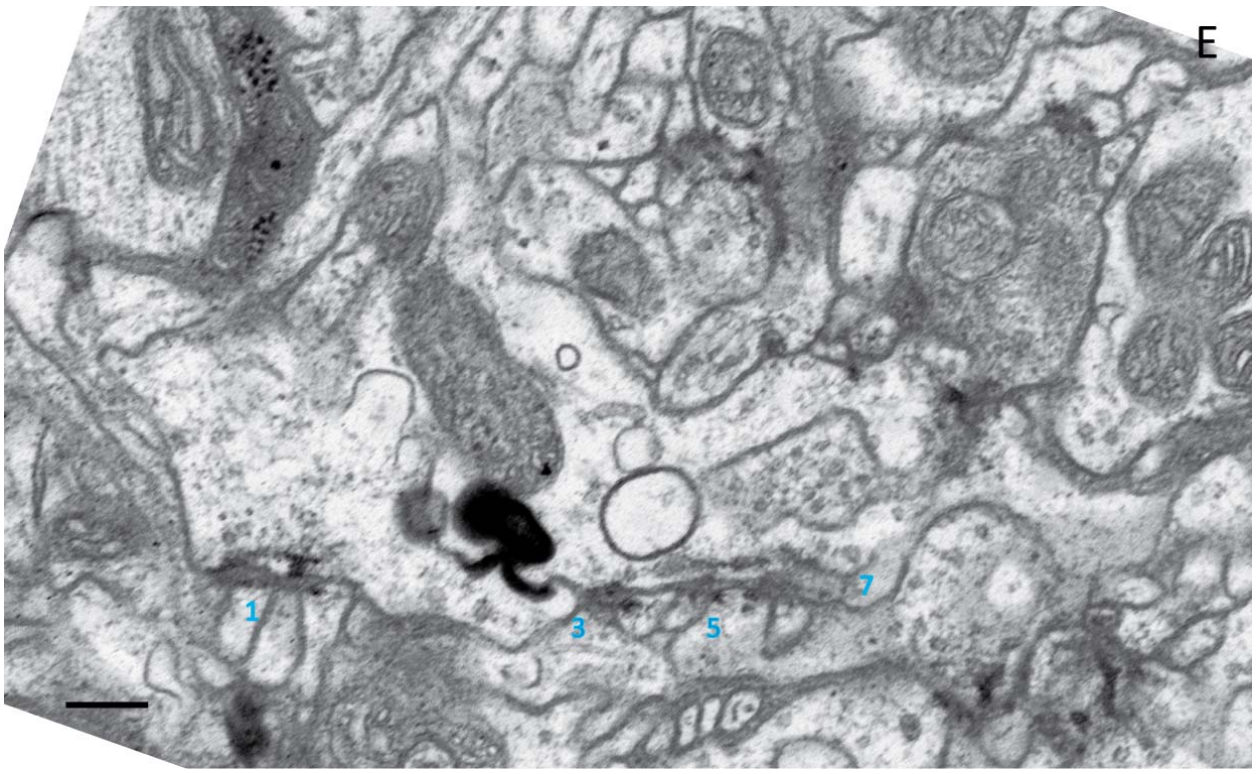

Figure 5: Stack 2 consists of five successive aligned images. The cell in the center was analyzed (marked in A), has a perimeter of averagely 6.4(±1.3)µm (n=5), covers an area of 1.2 (±0.3)µm^2(n=5) and has a depth of minimal 350nm (n=5). Notice that synapse no. 2 (in A and B) is included into analysis (similar stereotypy, see table). The perimeter is of this cell is larger than in cell 1, despite nearly the same area. This difference is caused by greater membranous surface irregularities verses the round- shaped cell in stack 1. The cell is surrounded by a number of maximal 27 cells, 13 of them connect to the investigated tangential cell. The synaptic sites (arrows in A) can be identified from the areas of electron dense material (appears darker in the images). All identified synapses were numbered and listed consecutively with corresponding features in table 2. Magnification: 50.000X, scale bar 0.2µm.

4.2.2 SYNAPSES

The active zone is associated with vesicles and pointed by regions of highly organized electron-dense material (appears darker in the images) docked to the presynaptic membrane. These clusters can form T- shaped or different spherical-shaped structures in cross- sectioned active zones. Opposite the synaptic cleft often occur postsynaptic densities.

4.2.2.1 TYPICAL SYNAPTIC ARCHITECTURE AT LPTCS- NEURITES IN DROSOPHILA`S BRAIN

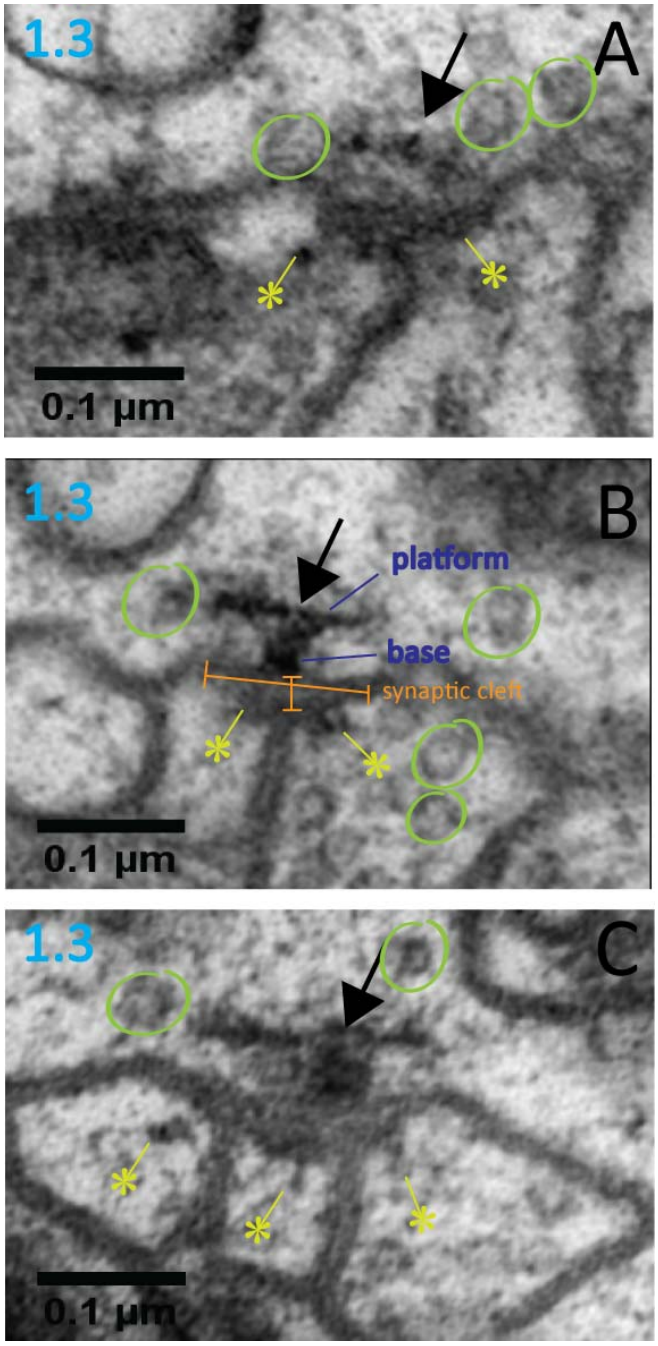

Figure 6: **Close-up of a typical synapse** (no. 1.3) in *D. melanogaster*. Scale bar 100nm.

The commonest type of synapse of the investigated sections, the T bar, is composed of a body (base) and a platform on the top (arrow, Figure 6). The base is connected by a synaptic cleft (lines) to 1 to 3 other postsynaptic neuronal cells, monads, dyads and triads were found. With regard to the small amount of images, often probably not all terminals could be traced and also when the synaptic site was cut transversally some could not clearly be identified. The average length of the platforms, measured at the largest point per synapse is 120.8 (±30.4)nm (n=4) in stack 1, but can span a width up to 333nm (Figure 10), thus occur at four successive sections, each of which is approximately 70 nm. The great size of platforms secures a relatively easy and unambiguous identification of the type, because they can be found within two to five sections (exceptional no. 2.3, because of a large distance to the prior slice, the platform occurred only once, Figure 11)

The analysis of stack 2 revealed an average length of platforms of 224.7(±73.4)nm (n=6), measured by the highest values per synapse. This great difference is explained by the number of detected platforms per stack. Whereas along

stack 1 eight profiles of platforms were revealed, in stack 2, almost the double amount of fifteen platforms was detected. The shown synapse (Figure 6) innervates three different cells and is thus called triad, seen in the postsynaptic densities (asterisk). The platform has a width of 155nm, along with a base, occurring in B and C, of 27nm in height and 48nm in width, at its thickest point (see all determinations of measurements in Scheme 3, Methods). Eight synaptic vesicles with a size ranging from 33 to 39nm, occur in the proximity of the active zone. Notice the synaptic vesicles (circles in B) in the postsynaptic cell, which also indicate nearby presynaptic activity. This element of a multiple postsynaptic complex is probably functioning simultaneously as pre- and postsynaptic site. The synaptic cleft between corresponding terminals spans 15nm to 33nm, with the greatest distance directly under the bar. There the length of the synaptic cleft is approximately 162nm.

The average height of the synaptic dense bars of the averaged values of each synaptic site, was 35.3(±8.1)nm (n=9) measured in terminal 1 and 42.6(±11.4)nm (n=6) in terminal 2.

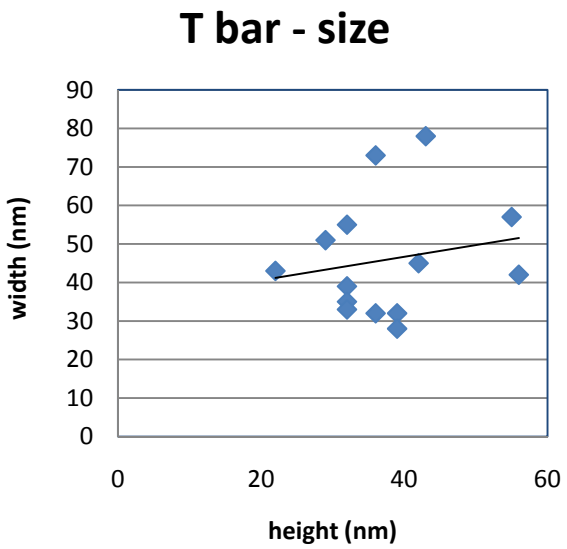

Figure 7: Diagram of correlation between averaged heights to averaged widths per synapse. (Trend line: y = 0.3044x + 34.513), R^2=0.0346

A correlation between width and height within a T bar is not obvious, but between the average values per synaptic sites, a trend can be noticed. (Figure 7) The coefficient of determination R^2 is too small to obtain a proportional correlation. Generally, the higher the dense base the wider it is. An average width of T-shaped synapses of the average values of each synapse is 37.0(±10.4)nm (n=9) for synapses in terminal 1 and 61.6(±35.4)nm(n=5) for synapses in terminal 2. The high standard deviation may be explained occasional laterally cuts through the center of the active zone (no. (2.2), 2.1).

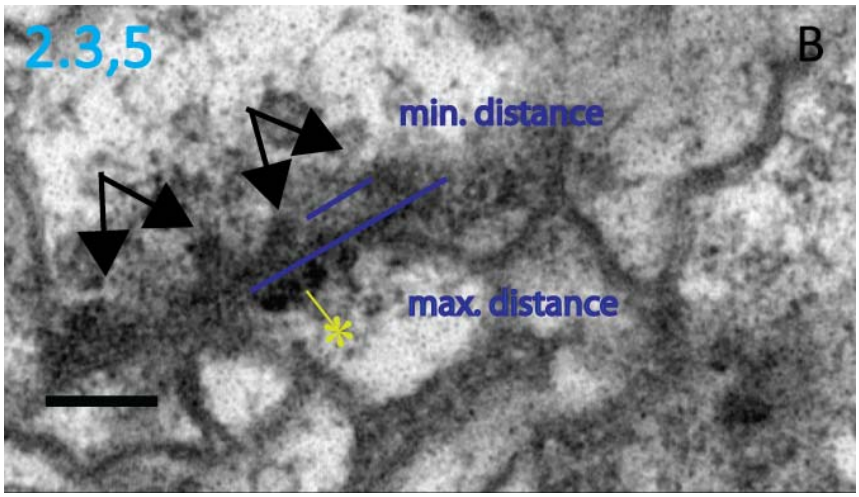

Figure 8: Close-up of a laterally cut T bar. (no. 2.3, 2.5) Two cube-like to longish synaptic sites occur. Scale bar 100nm

When laterally cut through the endings (arrows, Figure 8), two cube-like or longish circles appear in a minimum distance (facing sides of the circles) was measured at three synaptic sites (no. 2.3, 2.5, 1.9) and is averagely 70.3(±11.0)nm (n=3) with a maximum distance is averagely 183.7(±6.0)nm (n=3). Thus the laterally cut sides are averagely 56.6 (n=3) each with a height of averagely 36.5nm (n=3). These cases are marked in the table column `specials`.

15 of 17 identified synaptic sites among the two analyzed terminals (incl. no.2.2) were of that T -shaped type. The two other synaptic sites showed only their postsynaptic sites and could not be clearly identified. In three cases (no.1.1, 1.6, 1.7) the typical form of a `T` was not visible because of the missing continuing section, but they measure values, which are comparable with those of clearly seen T bars, thus were counted for this type (Figure 9). According to the dense body with the largest platform (Figure 11), only three sections traced the strand of filaments. This is because between slice B and C exists a larger distance than 70nm, visible at the mitochondria in the center of the cell. Whereas between slice A and B only a little difference can be seen, at slice C already the last part of the organelle occurs. However, the appearing length of the platform depends on the plane of sectioning. The platform with an exceptionally high length of 333nm is likely to be the longest point of the T bar. This synaptic site would appear at four, almost five cut sections, when rotated through 90 degree. The correspondingly high width of this T bar of 175nm indicates that it was laterally cut. This synaptic site nicely showed filaments (arrowheads, Figure10), building the topside of the T-shaped body and fixing onto the membrane beside the synaptic body. Among a small series of sections a great variety

of synaptic profiles could be revealed and shows several appearances caused by different planes of sectioning (see Figure 5, in introduction).

4.2.2.2 HIGH DENSITY OF SYNAPSES ON THE POSTSYNAPTIC SITE

Despite the occurrence of multiple synaptic contacts, one region within the observed cells was rather monadic as it had the unique appearance of input- supplying synaptic contacts along the cell 1. Figure 9 shows the main input region within stack 1, here four different synaptic sites contact to the cell, with one (no.1.5) also contacting to multiple neighboring elements.

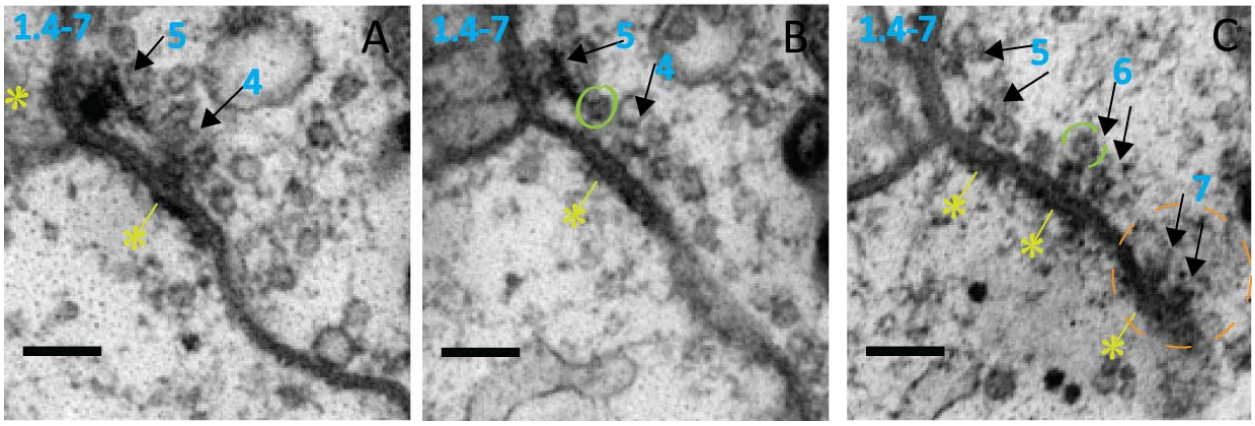

Figure 9: Close-up of (no. 1.4, 1.5, 1.6 and 1.7). Scale bar: 100nm

In Figure 9 (A), synapse no. 1.5 is seen as a tangential cut through the active zone, with a smaller base in the next section (B) and with separated endings in the third section (C). This example nicely shows a cut through the synapse (Figure 5: Introduction). The platform, also seen in the neighboring dense body, always serves as a great indicator, as well as surrounding and tethering vesicles nicely show an exemplar of a T bar. The average height of the base is 39nm, along with the average width of 32nm. The two dividing endings are smaller than the first section revealed, but as high as in B, with 37nm. According to the synapses no. 1.6 and no. 1.7, which occurred in the last sections, were thus first cut in nearly the same separated region. Two single electron dense synaptic vesicles (semi-circle) are involved and indicate synaptic activity. Also slight electron- dense material around the active zone (orange circle) and a recognizable widened membrane is visible. Three synaptic densities occurred at the opposite

membrane side of the investigated cell, belonging to three different presynaptic sites (C, asterisks). The synaptic sites are spread through an approximately 367 nm long region, with a slightly widened membrane of approximately 20nm. Each pair of presynaptic densities and the separated PSD opposite them are near to each other indicate a cut through the separating endings of electron dense material (Figure 5, Introduction). The pairs measure nearly the same height of 39nm(no.1.6) and 32nm(no.1.7) and a width of 28nm(no.1.6) and 33nm(no.1.7). A pair measures similar values, compared with each other. The neighboring synapse no 2.4., which appeared in the previous section (B), speaks in favor with the current structures by measuring a height of 35nm and a width of 30nm. Here, one can be sure to see a T bar, because of the platform visible in A. Thus the matching size of the dense bars, the paired size of presynaptic dense bodies and the separated postsynaptic structures can be assumed to be related to a T bar. But still, it would need the continuing section to evidence this and thus other synaptic site formations can be possible.

4.2.2.3 INPUT AND OUTPUT

Opaque, electron- dense material exists within the cleft and the cytoplasmic face of the cell to which it is connected. This gap is bridged by chemical transmitters diffusing from the release site, the presynaptic side to receptors on the postsynaptic side. The criterion as to weather a process is pre- or postsynaptic and thus an input or output- site is purely of morphological nature. That is, the processes appearing beneath the presynaptic density was assumed to be postsynaptic. The determination in the tables, weather input or output, is always based on the traced neuron. So a presynaptic electron dense body at the membrane in the traced cell provides. In cell 1, 9 presynaptic (output) contacts were found within ten synaptic sites in total. In cell 2, 14 presynaptic (output) contacts were found within seven synaptic sites. Cell1 Nine presynaptic contacts (output) and one postsynaptic (input) contact in an area of 1.3(±0.05)μm^2 (n=3)were found. Additionally synapse no.1.2 is probably also postsynaptic, because a PSD could be detected. The presynaptic density was covered by another cell.

Cell 2: 14 presynaptic contacts in an area of 1.2 (±0.3) μm^2 (n=5) were found. Only one structure is similar to a PSD, but did not show any presynaptic density.

4.2.2.4 CONNECTIVE TERMINALS

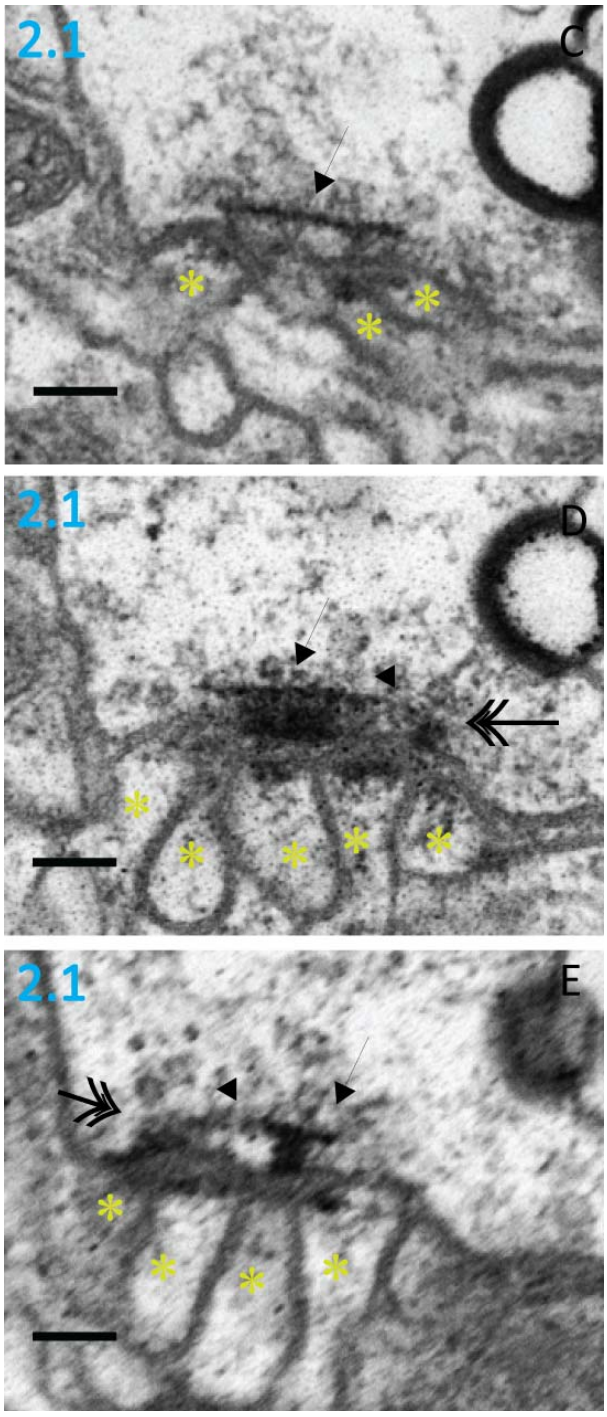

In 9 out of 15 unambiguously identified chemical synapses the cells were presynaptic to multiple postsynaptic targets (Figure 10). Often, a number of small accumulated terminals are docked onto the synaptic site of the traced tangential (see no. 1.5, 1.8, 2.1 (Figure 10), 2.3,2.5 (Figure 11)). Four dyad synapses and five triad synapses were found. Also eight monad synapses, where three (no.1.4, 1.6, 1.7) of them connected to the same cell 1, were identified. Two were identified only by their PSD. Also noted, but not counted for analysis, was synapse no. 1.2, which receives input from a remarkable dark occurring cell. This is caused firstly by a high amount of proteins within the cell and secondly by a huge amount of synaptic vesicles, a singularity within the traced cells.

Figure 10: Multiple contact type of three elements (asterisks) which connect to the observed terminal, indicated by postsynaptic densities. Scale bar 100nm. This T- bar (arrow) had the overall largest platform of 333nm and the widest base of 175nm.
A small spacing between the platform and the base can be seen in D. The height of 46nm is slightly above an average value of 42.2(±11.3)nm within this stack.

At image one the dense base did not occur, but the platform is clearly visible. At the two lower images, two electron densities (double arrow) at the presynaptic membrane can be seen, first on the right side (D) and then on the left side (E). Both, the position of the projections on the membrane and the exceptional wide dense-bar, in D, signal a cut sagittal through the active zone. Especially in D, the widened synaptic membrane of an also overall highest length of 407nm and a height of 24nm can be noticed by an almost unstained cleft between the two layers. According to both of the cells, the most observed synaptic sites were of the type multiple-contact synapse (Lamparter et al., 1969; Meinertzhagen, 1984), at which output is given upon those clusters of multiple postsynaptic elements (Fischbach and Dittrich, 1989). These observations of synaptic sites connected to a great cluster were made in case of synapse no.1.1, 1.3, 1.5, 1.8, 2.1, 2.3 and 2.5, see Figure 8 or Figure 10. The amount of terminals connected to synaptic sites was determined by postsynaptic densities. It can be assumed that the number of involved terminals is variable. In total, output was provided to 9 terminals from cell 1 and to 14 terminals from cell 2. Despite the smaller number of detected synapses in cell 2, presynaptic synapses were found than in cell 1.

4.2.2.5 SYNAPTIC VESICLES

Criteria of chemical synapses, such as T-bars, are vesicles which can be found cluster around that site, defined as output giving site. Generally, discovered clusters of synaptic vesicles indicate synaptic activity nearby. Round vesicles are attached to the presynaptic site, several of them occurred with a little of electron- dense material (Figure 12). In several cases docked variants were found (circle in D). The most abundant vesicles are of a round type with a clear or granular core and show a darker surface. An overall vesicle size in the range of averagely 28-41nm was observed. Up to 25 involved synaptic vesicles at one synapse could be detected, counted along the whole presynaptic dense body. The average size is 34.7(±4.7)nm (n=16) found in terminal 1 and 33.6(±3.9)nm (n=17) found in terminal 2, which is very similar.

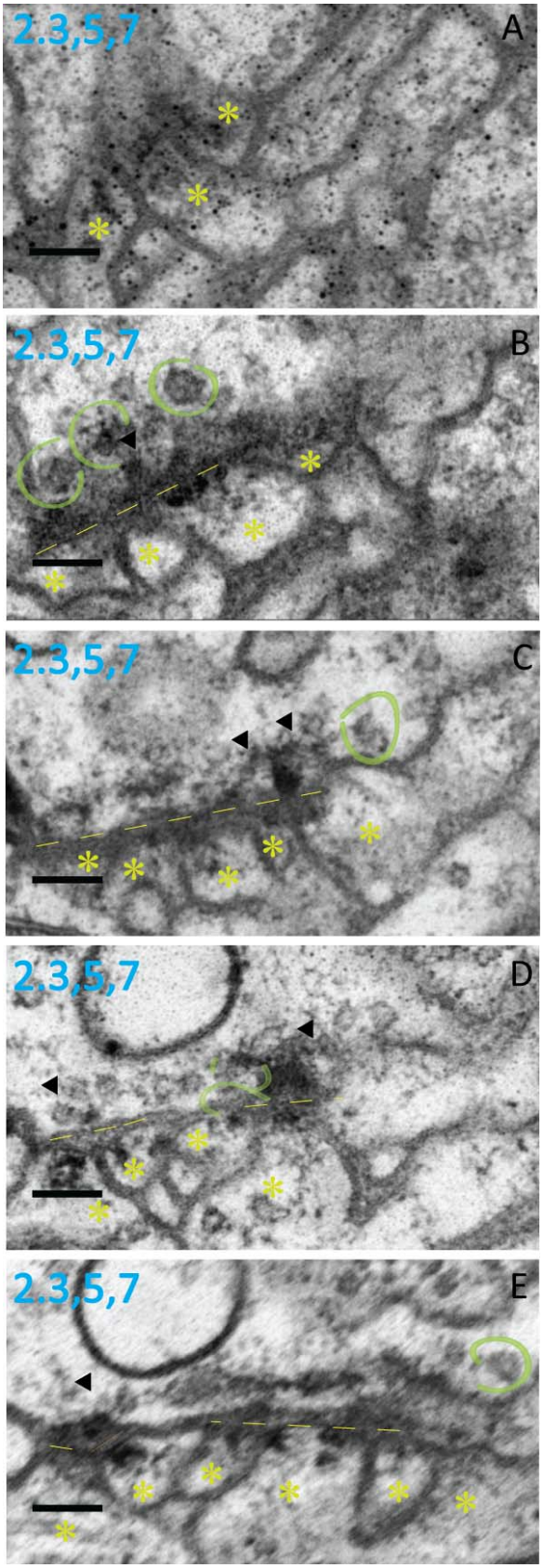

Figure 11: Synaptic sites connect to a multiple element clusters (asterisks). Filament strand marked with arrowheads and vesicle with circles. The dashed lines point at continuous membranes. Scale bar: 100nm.

A high electron density line occurred in D (no. 2.7), 131nm above the membrane, too high for a T-shaped synaptic site ranging 42.2(±11.3)nm within this stack. On the upper side occur two clear core vesicles, speaking in favor for the presence of a synapse. Also the occurrence of the new single terminal is likely to make a new connection. The following section evidenced the first cut of a T- bar synapse by a darker and larger platform and longish postsynaptic structures spread within three different terminals. In this special case the height of 47nm describes only the distance from membrane to platform and is in the range of the average height of a T bar. The widened membrane of 20nm is within average of this stack. Two more vesicles in the region of activity coincide with that. Scale bar 1nm.

4.2.2.6 MEMBRANE

The active zone is separated from the postsynaptic process with a synaptic cleft which possesses a web-like substance to closely align the separated membranes. Electron micrographs nicely visualize this pattern. In this study the average widening is 20.4(±4.8)nm at synaptic sites in stack 2 and 24.3(±6.6)nm for those in stack 1. Measured was the thickest point. One of the exceptional wide matrixes of 34nm was obtained from a T- bar which was tangentially cut to the active zone and thus offering its center (Figure 13). Consequently, it can be assumed that the highest activity, probably in the middle of this synaptic body is in favor of the functional aspects or even causes the thickening of the membrane, which is made of structural integrated proteins. Also locations of serially arranged synaptic densities (Figure 9 and Figure 12) showed this great expansion and seem to connect it. In these cases only the area, which belongs to connected terminals, indicated by postsynaptic densities, was measured.

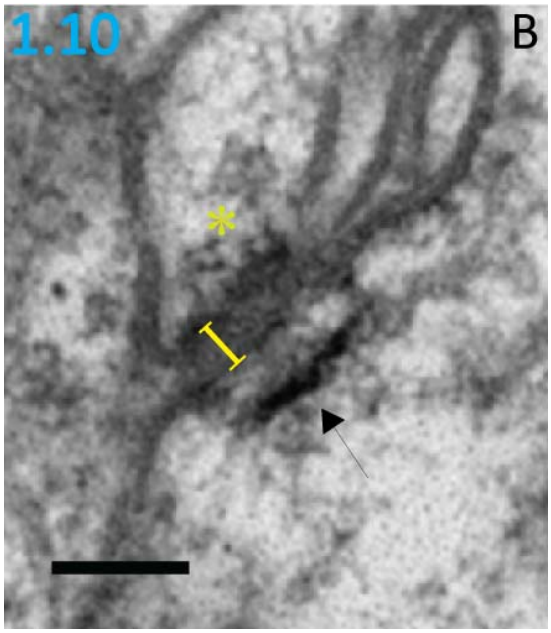

Figure 12: Monadic synapse with a wide membrane, which was cut through the middle of the active zone. The marked membrane is 34nm. The presynaptic site (arrow) reveals a pedestal of 36 in height and 32nm in width, which is thinner than averagely measured along all bases. The prior and the successive image did not show parts of the base. Remember the certainly larger distance between sections B and C, thus only the following image slightly showed continuing electron dense strands, attached at the membrane. Also the output terminal was only fully

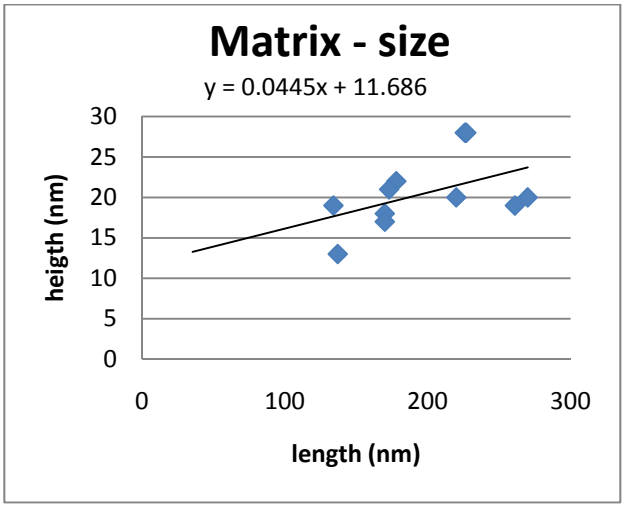

Figure: 13: the longer the membrane the wider it is. $R^2 = 0.2205$

4.2.2.7 POSTSYNAPTIC DENSITY (PSD) AND SPEZIALISATIONS

Two different PSD were found in this study and measured among both of the cells (see table 3). The wide- type (Figure right column) has a height of 14.9(±4.8)nm (n=31) and width of 47.8(±28.9)nm (n=31). The long- type(Figure left column) has a height of 30.0(±11.2)nm (n=34) and a width of 16.2(±7.9)nm (n=34). In most cases, only PSDs of one of these types were detected at one synaptic site, or otherwise at least a priority can be seen. The quantity of the appearance of wide- type and long- type PSDs is similar and no correlation to number of terminating elements, weather input or output to the cell or type of presynaptic dense body can be assessed.

At six wide type PSD out of 65 PSDs occurred specializations with an elongated appearance and a width of 10.2(±3.6)nm (n=17) and a height of 53.6(±16.1)nm (n=17). Up to four of these specializations were found at wide PSD. In small multiple contact elements these elongations branch almost through the entire cytoplasm. Signaling molecules, regulatory proteins and ion channels are known to possess in the postsynaptic membrane (reviewed by Kennedy, 1993 Kennedy, 1997).

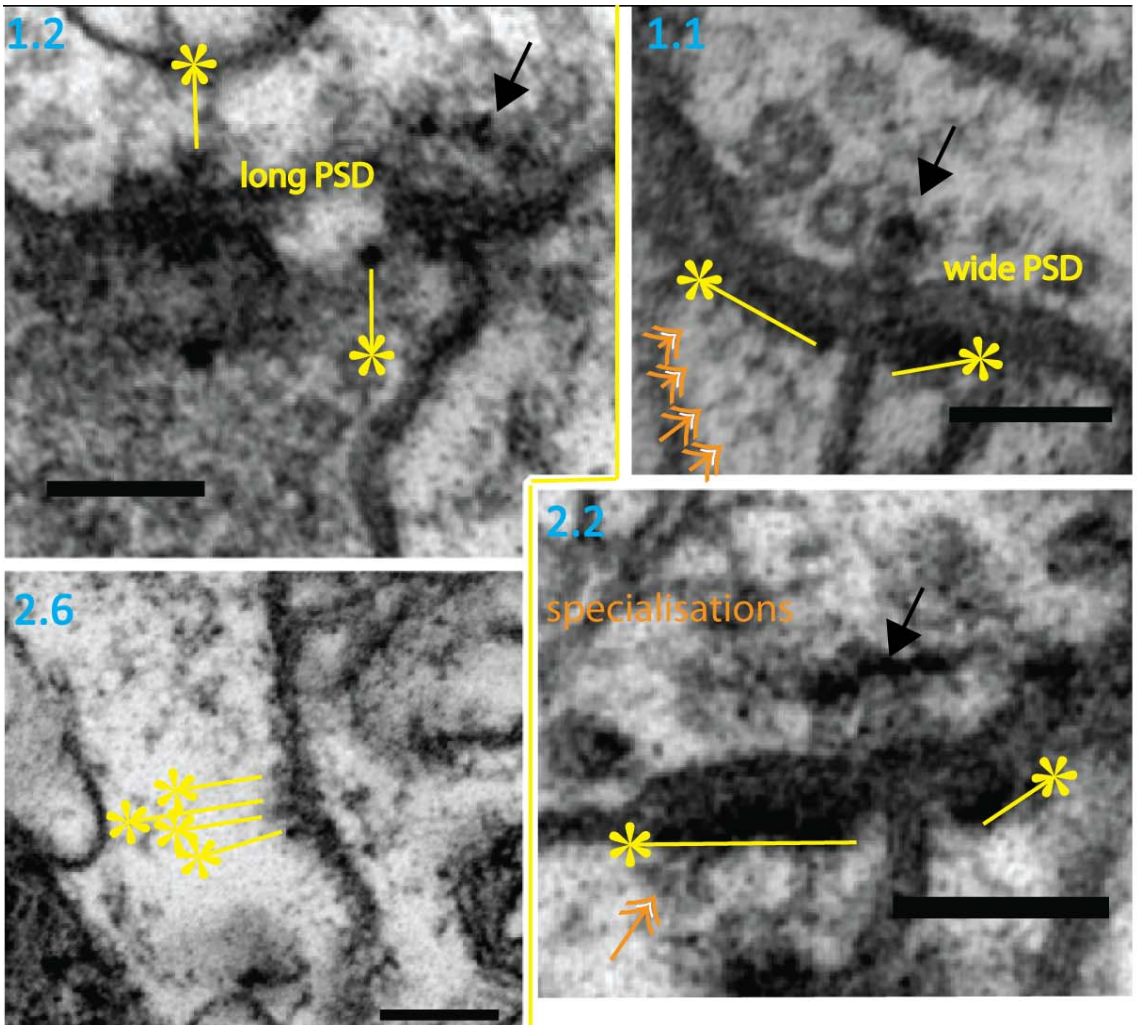

Figure 14: PSD AND SPECIALISATIONS

According to a slight platform-like projection, visible in the previous section synapse no.1.1 may also belong to the T-shaped synapses, but it cannot be evidenced.

This dyad synapse, has two prominent wide type postsynaptic densities, one of a height of 23nm and a width of 42nm and a second of a height of 15nm and a width of 82nm, the latter shows four longish specializations, which almost branch through the entire cytoplasm. These elongations have a constant width of 8 to 9 nm, in contrast to the height, which is graded from 21 to 65nm. Also synapse no. 1.2 likely is a T bar, but not evidenced because the presynaptic site, within a dark content and is half- covered by a new appearing terminal. It shows has a longish appearance. Synapse no.2.6 was an exclusive case, because it shows no presynaptic electron densities. Four long PSD were measured. Scale bars: 100nm

TABLE 1 (stack 1) no evidence* averages of the highes values** averages of the highes values of average values per synapse*** (height= distance membran)

cell 1		section	synapse														
perimeter(µm)	aera (µm²)		no	type	connective	size (nm)			location	in/output	pre		post	matrix		specials
					terminals	platform	height	width	terminal		vesicles	diameter		length	height	
4.4	1.25	A	1	T bar	dyad	145	24	40	main	output	1	49	density	137	29	
4.8	1.35	B		*			29	65			0	*		200	28	only platform
4.8	1.3	C					35	48			5	35		302	33	
4.7 (±0.2)	**1.3 (±0.1)**	av/syn					29.3	51			6			213	30	
		A	2	*	monad	*	*	*	main	input	0	*	density	124	15	postsynaptic
		av/syn														
		A	3	T bar	triad	95	30		main	output	5	39	density	80	15	
		B				110	39	29			2	33		162	33	vesicles
		C				155	27	48			3	34		97	18	postsynaptic
		av/syn					32	38.5			10			113	22	
		A	4	T bar	monad	71	35	30	main	input	5	33	density	183	19	4,5,6,7
		B					29	38			4	30		157	22	connected matrix
		av/syn					32	34			9			170	20.5	
		A	5	T bar	triad	95	45	45	main	input	6	35	density	177	21	input
		B				88	37	28			4	31		141	19	multiple contact
		C					37	22			4	33		267	20	2 endings
							37	32								
		av/syn					39	32			14			195	20	
		C	6	T bar	monad		39	28	main	input	1	33	density	170	18	2 endings
							39	28								distance=18nm
		av/syn					39	28			1			170	18	
		C	7	T bar	monad		32	33	main	input	1	30	density	178	22	2 endings
							32	32								distance: 22nm
		av/syn					32	33			1			178	22	
		A	8	T bar	dyad		56	42	main	output	4	34	density	170	17	oblique- cut
		av/syn					56	42			4			170	17	
		A	9	T bar	monad		22	43	main	output	1	34	density	96	19	lateral view
		B												172	20	distance: min.: 71
		av/syn					22	43			1			134	19.5	
		B	10	T bar	monad	138	36	32	main	output	1	32	density	230	34	mid -cut
		C									1	40		222	22	
		av/syn					36	32			2			226	28	
		TOTAL	**10**		**16.0**	**120.8**	**35.3**	**37.0**		**5 to 5**	**48.0**	**34.7**		**174.3**	**21.9**	
		stdev(total)				30.4	8.1	10.4				4.7		56.9	6.0	
						**	***	***				**		***	***	

TABLE 2 (stack 2) no evidence* averages of the highes values** averages of the highes values of average values per syn (height= distance membran)

cell 2 perimeter	aera (µm²)	section	no	synapse type	connective	size			location	in/output	pre		post	matrix		specials
					terminals	platform	height	width	terminal		vesicles	diameter		lengh	height	
4.8	0.9	A	1	T bar	triad	99	26	50	main	output	3	30	density	153	21	
5.6	1.1	B				88	60	45			4	28		135	13	
6.0	1.2	C				230	36				4	39		325	20	
7.7	1.5	D				333	46	175			10	30		407	24	
7.7	1.6	E				211	47	43			4	35		287	19	
		av/syn					43	78.25			25			261.4	19.4	
6.4	1.2	A	(2)	T bar	triad	245	38	87	different	output	4	33	density	277	19	
1.3	**0.3**	B				88	34	60	cell		4	34		263	22	
		av/syn					36	73.5			8			270	20.5	
		B	3	T bar	dyad		45	95	main	output	2	39	density	197	26	distance:
							33	66								min.:81
		C				196	37				1	28		258	30	max.:178
		D					25	28			3	33		133	23	
		E					20	30						124	22	lateral view
		av/syn					32	55			6			227.5	28	
		C	4	T bar	monad	207	55	48	main	output	3	33	density	141	13	
		D				201	56	66			3	31		133	14	
							55.5	57			8			137	13.5	
		B	5	T bar	dyad		36	35	main	output	1	41	density	174	17	distance:
							41	37								min.:59
		C				86	60	45			2	33		99	25	max.:190
		D				153	43	71			2	33		202	17	
		E				186	30	35			0			218	25	
		av/syn					42	44.6			5			173.3	21	
		C	6	*	monad		20	10	main	input	0		density	100	12	postsynaptic
		D					19	9			0			126	14	
		av/syn									0					
		D	7	T bar	triad	118			main	output	2	39				
		E				181	47				2	32	density	222	20	
		av/syn					47				4			222	20	
		TOTAL	**7**		**15**	**224.7**	**42.6**	**61.6**		**1/6**		**33.6**		**215.2**	**20.4**	
		stdev			**±**	**73.4**	**11.4**	**35.4**				**3.9**		**82.1**	**4.7**	
						**	***	***						***	***	

DENSITY AND SPECIALISATIONS

	PSD (nm)				specialisation				PSD (nm)				specialisation	
	no	height	width	specials		height	width		no	height	width	specials	height	width
A	**1**	**21**	13		1	21	9	A	**1**	16	17		4 48	15
		23	12			29	8			**23**	19		65	16
		27	14			46	9	B		25	25		5 35	13
B		**17**	13			65	8	C		**26**	15		39	13
		24	8		2	64	7			13	24		6 47	11
C		15	**82**	no 1		70	5			17	21		59	13
		23	**42**			73	6			**25**	12			
A	**2**	**27**	17	input		69	15	D		18	52			
A	**3**	**25**	11		3	69	10			17	67			
		30	12			58	5			5	37	no 4		
B		19	**27**					A	**2**	14	64			
		9	**14**					A		14	23			
C		**29**	14							13	45			
		36	5							17	96			
		36	15							13	29	no 5		
A	**4**	11	**84**					D	**3**	**55**	35			
B		10	**16**							**35**	14			
A	**5**	13	**23**					E		**45**	36			
		11	**19**						**4**	**54**	36			
B		7	**19**							**52**	21			
C		14	**72**					B	**5**	22	84	no 6		
		15	**49**	no 2						22	25			
C	**6**	12	**99**	no 3						**23**	18			
C	**7**	8	**93**					C		**29**	19			
A	**8**	13	**41**							**21**	18			
		53	16					D		**27**	20			
A	**9**	**34**	12							22	43			
B		**22**	12					E		**41**	27			
		15	12							**40**	26			
B	**10**	18	**108**						**6**	**22**	8			
TOTAL										**29**	14			
long		**30**	**16.2**			**53.6**	**10.2**			**18**	5			
wide		**14.9**	**47.8**							**12**	8			
PSD									**7**	17	42			
										24	13			
stdev		11.2	7.88			16.1	3.64							
		4.83	28.9											
		long	wide											

bold: highest value = determination for long or wide PSD

5. DISCUSSION

The presented ultrastructural analysis first drew attention to the architecture and structural implementation of chemical synapses of lobula plate tangential cells in *Drosophila melanogaster* to gain information about possible structural differences presumably caused by different functional implementations.

5.1 EXPERIMENTAL REVIEW

Special attention was paid to the fixation step. Several very exact instructions had to be taken into account to obtain a clearly fixed specimen. The fast fixation by rapidly transferring the specimen into the fixative is necessary to secure the ultrastructure. *Drosophila melanogaster* has served as a standard model for a period of time, thus a fixative which has already been proven to be suitable was used. In general, one has to keep in mind that taking a fixative which fixes more variability, will deteriorate ultrastructure and thus the synapses which want to be seen. The postfixation with osmium tetroxide contrasted the membranous structures, thus that the investigated cell and all its surrounding terminals were seen. The cutting of the specimen block is an important, but challenging task. The thickness of a sections has to be thin enough (less than 100nm) to image it later on in the TEM, but the ultrastructure of the specimen still has to be preserved. Influences such as air flow or little shakings at the device can change the precise position and probably cause different thickness of slices. Each missing slice or variable slice thickness changes the significance of revealed images, meaning a statistical analysis among a number of images can only be revealed from a section thickness which is exactly known. The quantity of successive images which were analyzed, were mainly caused by loss of pictures, either because of poor work during the cutting process or in some cases when the electron beam in the TEM burned the slice, caused by a low quality polioform film on the slotgrid. Retrospectively, the slotgrid between the two investigated ones was not investigable because

of a broken polioform film. Thus, stack 1 and stack 2 were obtained and contain the prior three and the latter five successive images each. Afterwards it was noticed that stack 2 did not locate in the same area, as previously thought when searching for the cells at the TEM.
When using the TEM the controlling was mainly done by Christoph Kapfer (MPI, Computational Neurobiology).

5.2 ANALYSIS REVIEW

A first stack of three successive images and a second stack of five images were of good quality and taken for analysis. The analyzed TEM images revealed a well-preserved ultrastructure of synapses, cell membranes as well as other cell organelles, evidencing a proper fixation. Only a small amount of ruptured mitochondria were detected (stack 2, black circle), but this did not distort the validity of the images. Some synaptic sites we already detected when following the image stack with the camera mounted at the TEM. But most of the listed synapses were found afterwards, when the aligned images were studied in detail. Referring to the cross-sectioned plane, which was observed from the cells, it was possible to retrieve the synaptic profile on the continuing image. Otherwise it was assumed that the synaptic profile ended between the sections. A first indicator of the presence of a synapse is an area which appears darker.

Analysis criteria for synapses were the presence of synaptic vesicles associated with the presynaptic membrane, a widened synaptic cleft, the presence of a dense body bar or T- bar, PSDs and its specializations. Using the image analysis software (Fiji), the diameter and perimeter of the traced cells, amount, size and types of synapses as well as the diameter of vesicles, which surround the presynaptic electron dense body in a distance of maximal 50nm were measured.

5.3 RELATIVE AMOUNT OF SYNAPTIC SITES

Cell 1, consist of three successive images. The average perimeter of the cell 1 is 4.7 (±0.2)µm (n=3)and the average area 1.3 (±0.05)µm^2(n=3). Cell 2 consists of five successive images, with an average perimeter of 6.4 (±1.3) µm (n=5) and an average area of 1.2 (±0.3) µm^2 (n=5).
Each image, which was investigated for synaptic sites, has a distance of approximately 70nm to the following one. The area of both of the cells is almost the same, but the total perimeter of cell 2 is higher than cell 1. Despite this greater surface area, ten synaptic sites were found in cell 1 and only seven in cell 2. Additionally, two more sections were revealed of cell 2, reminding that between slice B and slice 3 a greater distance than 70nm was noticed. Thus, according to the corresponding surface of the traced cells, cell 1 reveals an even greater number of synapses per surface area (excl. no.2.2).
10 synapses in an area of 1.3(±0.05)µm^2 (n=3) for cell 1 and 7 synapses in an area of 1.2 (±0.3) µm^2 (n=5) were detected. Cell1 showed nine presynaptic contacts (output) and one postsynaptic (input) contact in an area of 1.3(±0.05)µm^2 (n=3). Additionally synapse no.1.2 is probably also postsynaptic, because a PSD could be detected. The presynaptic density was covered by another cell. Cell 2 showed 14 presynaptic contacts in an area of 1.2 (±0.3) µm^2 (n=5). Only one structure which is similar to a PSD but did not show any presynaptic density

5.4 DETECTION OF STEREOTYPY

A high morphological stereotypy of T- bars (Trujillo-Cenoz, 1965; Boschek, 1971) in *Drosophila melanogaster* was found. 15 of 17 identified synaptic sites among the two analyzed terminals were of that type. Two showed only their postsynaptic sites and could not be clearly identified. In three cases (no.1.1, 1.6, 1.7) the typical form of a `T` was not visible because of the missing continuing section, but they measure values which are comparable with those of clearly seen T bars, thus were counted for this type.

The number of synaptic profiles of the investigated volume within the stack, according to the T – shaped synaptic sites is high. The average platform length of the highest values per synapse is 120.8(±30.4)nm (n=4) on T bars among cell 1 and 224.7(±75)nm (n=6) among cell 2. In cell 2 a higher number of images revealed the platform. However, the appearing length of the platform depends on the plane of sectioning. The longest one which was probably laterally cut is 333nm (no.2.1). The average height of the synaptic dense bars of the averaged values of each synaptic site, was 35.3(±8.1)nm (n=9) measured in cell 1 and 42.6(±11.4)nm (n=6) in cell 2. An average width of T-shaped synapses is 37.0(±10.4)nm (n=9) for synapses in cell 1 and 61.6(±35.4)nm (n=5) for synapses in cell 2.

The average height of postsynaptic synaptic sites (at the output of the investigated cells) of the average values of each synapse is 35.5 (±4.5)nm (n=4), along with a width of 32(±6.29)nm(n=4).
A great difference is visible according to the width, but with regard to the high standard deviation not clarified. Two of the input cells are thought to be cut at the very start of the T bar, which was measured at three synaptic sites ranging from 28 to 33nm. The distance of these endings mounted in one synaptic site was averagely 20nm. The shown T bars which were laterally cut, had an average minimum distance of 70.3(±11.0)nm (n=3) with a maximum distance of averagely 183.7(±6.0)nm (n=3). Thus the laterally cut sides are averagely 56.6 (n=3) ,each , with a height of averagely 36.5nm (n=3).
The here obtained measurements, analyzed from different planes of sectioning can serve for further studies to reveal this T bar type. Even sections which cannot show the whole synaptic body or platform can be analyzed and classified according to these findings.
Among a small series of sections a great variety of synaptic profiles could be revealed and shows several appearances caused by different planes of sectioning.

5.5 MULTIPLE CONNECTIONS

Meinerzhagen (1984) found that within photoreceptors synapses can connect up to four neurons. This stereotypy in connections can be excluded within the lobula plate. Typical postsynaptic formations, like cristernae and capitates projections which were found in photoreceptors were also not obvious.

Among two of these postsynaptic connections only postsynaptic structures were visible.

Nevertheless the size of both of the cells is similar, also in terms of a varying size within the same cell and a similar amount of synapses was expectable, the function may be the analog.

5.6. PSD

The different shapes of PSD are maybe caused by different molecules, which are involved in the synaptic signaling process, but according to that no preferred shape of PSD was found.

Synapses in vertebrates can be ultrastructural classified into asymmetric and symmetric synapses (Gray, Colonnier), the previous can be distinguished by a thickened PSD and a presynaptic site surrounded by spherical or round vesicles. In contrast, symmetric synapses mainly contain pleiomorphic vesicles and contain no prominent PSD. Here, exclusively prominent PSDs of an average size, almost as high as the presynaptic density, were detected at all analyzed synapses. Thus, this could indicate the presence of an asymmetrical synaptic type, which is present within excitatory transmitter exchange. But for all, that the majority of synapses in the fly is the T bar this model cannot suggest a functional difference.

5.7 RELEVANCE FOR MOTION VISION

The aim of this study was to investigate the ultrastructur of chemical synapses at LPTCs. We focused a possible structural difference among 17 synaptic connections within the LPTCs to clarify if ultrastructure and synaptic organization can indicate what type of transmitter exchange is present onto LTCPs.

It is thought, that LPTCs compute local motion vectors (Reichardt, 1961; Borst and Egelhaaf, 1989), as the output of an array of Reichardt detectors (Reichardt, 1961).

The summation step of local motion signals is thought be realized at the dendrites of direction selective VS and HS cells. GABAeric and cholineric input to the receptors on the dendrites could there function as mirror symmetrical subunits of the Reichardt detector to turn the input signals into direction selectivity. The subtraction step could be realized by superposition of excitatory and inhibitory synaptic currents within the dendrtites of LPTCs. It is hoped to discover the underlying computational circuits of the reichardty-detector, and thus the mechanism of motion vision processing.

Recent findings suggest specific localizations of nicotinic- acetylcholine receptors (nAChRs) and y-aminobutyric- acid receptors (GABARs) at their dendrites at the lobula plate (Raghu et al., 2009). These two different types of receptors indicate that excitatory and inhibitory motion-sensitive elements with opposite preferred direction provide input from local motion detectors onto the fine dendritic branches of LPTCs (Raghu et al.2007, Raghu et al., 2009; Brotz and Borst, 1996).

According to that we can assume that both, GABAeric as well as cholineric synaptic sites were maybe found within the investigated tangential cells.

We found no prominent ultrastructural difference among characteristic elements of the investigated synapses. The majority of the analyzed chemical synaptic sites at both of the investigated tangential cells were T bars opposite to a prominent PSD. The appearance of presynaptic sites was relative constant among the cells. Two different types of postsynaptic densities were found, the long PSD and the wide PSD, but did not occur with a specific preference for one of these synaptic sites.

A study which compared GABAeric and non- GABAeric synaptic ultrastructure figured out that the type of clear core vesicles is much more present in regions of GABAeric transmitter exchange versus granular vesicles in non-GABA synapses (Hyun- Woo Oh et al., 2007). They observed more heterogeneity in vesicle size and morphological type in those, whereas

GABAeric synapses revealed a relatively constant diameter range of 20- 45 nm and a constant shape.

Among the investigated cells the clear core type and several granular vesicles at synaptic sites in were found. The overall size of involved vesicles is approximately 34nm, in a range of 28nm to 49 nm. According to this mentioned study it can be assumed that the present cells are of a non-GABAeric type. The term `granular` for vesicles in this study was determined by comparing the gray scale density with other vesicles in the cells and within the mentioned study of Hyun-Woo Oh et al. 2007. More evidence would be obtained by measuring all vesicles which are in the surroundings of synaptic sites and the determination of their gray scale values to distinguish between clear core and dark appearences.

The organization of synapses occurred highly variable by meanings of their function as input or output side within the same cells. Despite, LPTCs are thought to be postsynaptic in the lobula plate (J. Haag and A. Borst, 2003). Here, presumably LPTCs showed that, both presynaptic as well as postsynaptic connections are situated at the membranes within the LPTCs. Ten presynaptic (excl. no.2.2) and six postsynaptic connections were found. Two of these postsynaptic connections could not clearly be identified, because only postsynaptic structures were visible.

So far, only a few studies revealed an insight into the lobula plate at ultrastructural level (Strausfeld and Lee, 1991, K. Hausen et al., 1980, Gauck et al., 1997). At the fly *Calliphora* the existence of a chemical synapses between T4 and an HS cell dendrite (Strausfeld and Lee, 1991) and also chemical synaptic sites were proved on single VS, HS, Col A, and CH cells (Hausen et al., 1980; Gauck et al., 1997) was shown. By staining a specific cell type and analyzing the corresponding electron micrographs, knowledge about the synaptic organization on the marked neuron can be achieved.

From the presented stacks of three and five electron micrographs we cannot surely assign which neuronal cell type was investigated. Compared to surrounding cells the investigated cells are relatively large. Columnar neurons, which branch with their endings in that region, may have such a small diameter, but their size not exactly known and is probably highly variable.

Two columnar cells, T4 and T5, which branch in all different layers of the lobula plate (Fischbach and Dittrich, 1989) and responsed during visual motion stimulation (Buchner et al. 1984) are proposed to support input to LPTCs (Borst and Haag, 2002). These findings are based on the anatomical implementation from prior neuropiles onto the lobula plate.

5.8 FUTURE PROSPECT

The exact synaptic organization of the whole circuit is still not known, but is the hearts` desire of many neurobiologists. Therefore the uncovering of the underlying anatomical structure is essential. The invention a new electron microscope technique called *SBFSEM* (Serial block face Scanning Electron Microscope) invented by Denk and Horstmann (2004) combines ultra thin sectioning and high resolution EM- imaging. This is achieved by imaging of backscattered electrons which reveal the top view of a specimens -block with a given volume, after every discarded thin section. In combination of 3D computer-aided reconstructions it is feasible to trace and visualize even small structure as synapses. In future this will uncover complete neuronal circuits, such as the visual system implemented in the columns in the optic lobes in *Drosophila* or other species.

For investigating individual processes studying TEM images will still be indispensible to study distinct locations and ultrastructures of neuroanatomical complexity. Even further developments in preparation techniques, specific contrasting and in the advice itself is preferable. It preserves a smaller effort in cost, time and the flexibility of mentioned reasons above.

Ultrastructural electron microscopic studies with several functional approaches have a great power to throw light on the dark of the neuronal implementation of Motion Vision processing, being not only the flies but also the human’s most important sensory input system.

REFERENCES

Bausenwein, B, Fischbach, KF (1992). Activity labeling patterns in the medulla of Drosophila-melanogaster caused by motion stimuli. Cell Tissue Res, 270, 25-35.

Borst,A. (2009). Drosophila's View on Insect Vision. Current Biology *19*, R36-R47.

Borst,A. and Haag,J. (2002). Neural networks in the cockpit of the fly. J.Comp Physiol A Neuroethol.Sens.Neural Behav.Physiol *188*, 419-437.

Borst, A, Haag, J, Reiff, DF (2010). Fly motion vision. Annu Rev Neurosci, 33, 49-70.

Borst, A, Haag, J (2007). Optic flow processing in the cockpit of the fly. Cold Spring Harbor Monograph Series 49: 101-122

Borst, A (2009). Drosophila's view on insect vision. Curr Biol, 19, R36-R47.

Braitenberg, V (1970). Ordnung und Orientierung der Elemente im Sehsystem der Fliege. Kybernetik, 7, 235-242.

Briscoe, A. D. and Chittka, L. (2001). The Evolution of Color Vision in Insects. Annu. Rev. Entomol. 1. 46:471–510

Brotz, T. M. & Borst, A. (1996). Cholinergic and GABAergic receptors on fly tangential cells and their role in visual motion detection. Journal of Neurophysiology, 76, 1786-1799.

Brotz TM,.; Gundelfinger ED, Borst A, (2001) Cholinergic and GABAergic pathways in fly motion vision. BMC Neuroscience, 2

Cajal SR, Sanchez D (1915). Contribution al conocimiento de los centros nerviosos de los insectos. Parte I. Retina y centros opticos. Trab Lab Invest Biol Univ Madr 13: 1-168

Cardoso, S.H. (2001). Communication Between Nerve Cells

Denk W, Horstmann H (2004). Serial block face scanning electron microscopy to reconstruct three-dimensional tissue nanostructure. PLOS Biology 2: 1900-1909

Fischbach, KF, Dittrich, APM (1989). The Optic Lobe of Drosophila-Melanogaster .1. A Golgi analysis of Wild-Type Structure. Cell Tissue Res, 258, 441-475.

Haag, J, Wertz, A, Borst, A (2007). Integration of lobula plate output signals by DNOVS1, an identified premotor descending neuron. J Neurosci, 27, 1992-2000.

Haag, J, Wertz, A, Borst, A (2010). Central gating of fly optomotor response. Proc natl Acad Sci USA, 107, 20104-20109.

Hardie, RC (1979). Electro-physiological analysis of fly retina .1. Comparative properties of R1-6 and R7 and 8. J Comp Physiol, 129, 19-33.

Joesch, M, Plett, J, Borst, A, Reiff, DF (2008). Response properties of motion-sensitive visual interneurons in the lobula plate of Drosophila melanogaster. Curr Biol, 18, 368-374.

Jösch, M., Plett, J., Borst, A., & Reiff, D. F. (2008). Response properties of motion-sensitive visual interneurons in the lobula plate of Drosophila melanogaster. Current Biology, 18, 1-7.

Laughlin, SB, Osorio, D (1989). Mechanisms for neural signal enhancement in the blowfly compound eye. J Exp Biol, 144, 113-146.

Joesch, M, Schnell, B, Raghu, SV, Reiff, DF, Borst, A (2010). ON and OFF pathways in Drosophila motion vision. Nature, 468, 300-U186.

Kirschfeld, K (1973). Das neuronale Superpositionsauge. Fortschritte der Zoologie, 21, 228-257.

Meinertzhagen,I. (2008). The Organization of Invertebrate Brains: Cells, Synapses, and circuits. Journal of Morphology *269*, 1461.

Meinertzhagen,I.A. and O'Neil,S.D. (1991). Synaptic organization of columnar elements in the lamina of the wild type in Drosophila melanogaster. J.Comp Neurol. *305*, 232-263.

Meinertzhagen IA; Hu X (1996) Evidence for site selection during synaptogenesis: The surface distribution of synaptic sites in photoreceptor terminals of the flies Musca and Drosophila, CELLULAR AND MOLECULAR NEUROBIOLOGY, 16(6), 677-698

Meinertshagen, I. A. (1971). Erroneous Projection of Retinual Axons beneath a Dislocation in the Retinal Equator of Calliphora. Brain Research 41, 39-49.

Strausfeld, NJ (1976). Atlas of an insect brain. Springer: Berlin, Heidelberg.

Raghu,S.V., Jösch,M., Borst,A., and Reiff,D.F. (2007). Synaptic organization of lobula plate tangential cells in Drosophila: gamma-aminobutyric acid receptors and chemical release sites. Journal of Comparative Neurology *502*, 598-610.

Raghu,S.V., Jösch,M., Sigrist,S.J., Borst,A., and Reiff,D.F. (2009). Synaptic Organization of Lobula Plate Tangential Cells in Drosophila: D7 Cholinergic Receptors. Journal of Neurogenetics *23*, 200-209.

Rajashekhar,K.P. and Shamprasad,V.R. (2004). Golgi analysis of tangential neurons in the lobula plate of Drosophila melanogaster. Journal of Biosciences *29*, 93-104.

Ramón y Cajal. Recuerdos de mi vida. 1923. Madrid: Pueyo. / English trans.(1966) Recollections of my life. MIT Press. Ref Type: Serial (Book,Monograph)

Scott,E.K., Raabe,T., and Luo,L.Q. (2002). Structure of the vertical and horizontal system neurons of the lobula plate in Drosophila. Journal of Comparative Neurology *454*, 470-481.

Schnell, B, Joesch, M, Forstner, F, Raghu, SV, Otsuna, H, Ito, K, Borst, A, Reiff, DF (2010). Processing of horizontal optic flow in three visual interneurons of the Drosophila brain. J Neurophysiol, 103, 1646-1657.

Strausfeld, NJ; Lee, JK (1996) NEURONAL BASIS FOR PARALLEL VISUAL PROCESSING IN THE FLY. VISUAL NEUROSCIENCE, 7(1-2), 13-33

Strausfeld,N.J. (1976). Atlas of an insect brain. (Berlin, Heidelberg: Springer).

Strausfeld,N.J. (1984). Functional neuroanatomy of the blowfly's visual system. In Photoreception and vision in invertebrates, M. A. Ali, ed. Plenum Publishing Corporation), pp. 483-522.

Strausfeld,N.J. and Lee,J.K. (1991). Neuronal basis for parallel visual processing in the fly. Visual Neuroscience *7*, 13-33.

Takemura,S.Y., Lu,Z.Y., and Meinertzhagen,I.A. (2008). Synaptic circuits of the Drosophila optic lobe: The input terminals to the medulla. Journal of Comparative Neurology *509*, 493-513.

Wertz, A, Borst, A, Haag, J (2008). Nonlinear integration of binocular optic flow by DNOVS2, a descending neuron of the fly. J Neurosci, 28, 3131-3140.

Zhai RG, Bellen HJ. The architecture of the active zone in the presynaptic nerve terminal. Physiology (Bethesda) 2004;19:262–70.

Zhu, Y, Nern, A, Zipursky, SL, Frye, MA (2009). Peripheral visual circuits functionally segregate motion and phototaxis behaviors in the fly. Curr Biol, 19, 613-619.